

The Microstructure and Mechanical Properties of the Ball-Milled Al-Mn-Zr Alloys with Ce and Y Additions

Eshetu Mentesenot A., Lekeka Biniam B., Tasisa Dawit M., and Fenta Haftamu T.

Department of Advanced Materials Science, MISIS University, Russia

DOI: <https://dx.doi.org/10.51584/IJRIAS.2025.100900082>

Received: 28 August 2025; Accepted: 04 September 2025; Published: 22 October 2025

ABSTRACT

Mechanical alloying (MA), hot press sintering (HPS), and post-annealing were used to create high-performance Al-Mn-Zr-based quaternary alloys containing the rare earth (RE) elements Ce and Y. Three alloy compositions (Al-4Mn-1,2Zr, Al-4Mn-1,2Zr-0,6Y, and Al-4Mn-1,2Zr-0,6Ce (at.%)) were high energy ball milled for 10 h, consolidated at 350 °C or 450 °C and subsequently annealed at 350-450 °C for periods ranging from 15 minutes to 4 hours' analysis of crystallite size supported the extensive grain refinement during milling (16--20 nm), whereas compaction at temperatures at 450 caused a notable grain coarsening (up to 84 nm. SEM-EDS elemental mapping revealed precipitation free zones and intermetallic-rich zones, indicating precipitates formation during thermal processing. After milling, Al solid solution and Al₄Mn for Al-Mn-Zr and Al-Mn-Zr-Y alloys, Al₆Mn phase for Al-Mn-Zr-Ce alloy were revealed. After sintering Al₆Mn and Al₃Zr phases precipitated for all alloys studied.

According to the compression tests, the addition of Ce and Y to Al-Mn-Zr alloys varies in composition and heat treatment. Ce-containing alloys have high ultimate compression strength (UCS) and ductility, while Y-modified alloys balance strength and ductility. Annealing for 1-4 hours at 400°C gave maximum values for Al-4Mn-1,2Zr. The alloy also had maximum microhardness and macro-hardness after annealing (~430 HV and 370 HV) respectively. Annealing led to a rise in hardness for Ce and Y alloys from about (~ 250-280) HV to more than ~350 HV. Sintering pieces at 450 °C produced nearly the ideal density which shows an improved packing of the structure. Still, keeping the samples at 450°C for a long period following mild pressing caused the grains to become coarse and diminished the ability to restore their properties.

High alloyed Al-Mn-Zr based alloys exhibited superior strength properties and Y/Ce increased ductility. It is shown in the study that the MA-HPS process can successfully design high-performance Al alloys and has implications for lightweight parts.

INTRODUCTION

The hunt for high-performance materials that can survive extreme temperatures has prompted substantial research into advanced alloy systems, notably those based on aluminum [1]. Many engineers have paid close attention to aluminum-based alloys because of their remarkable features and ability to be used in a variety of ways. Because aluminum is light, has great strength and resists rust, it can effectively be mixed with other elements. Their useful qualities in mechanical, thermal and electrical areas allow them to be used in many fields., since the need for high-performance materials is increasing, it is becoming necessary to use alloying elements besides the typical manganese and zirconium. The performance of aluminum alloys might be improved using Cerium and Yttrium (Ce and Y) in the research.

Conventional aluminum alloys frequently fail to fulfill the demanding demands of increased temperature applications, necessitating the development of innovative alloy compositions and processing techniques to overcome these constraints [2] Mechanical alloying, a solid-state powder metallurgy process, has emerged as a potent tool for synthesizing complex alloy systems with higher microstructural control and better characteristics. This method allows production of homogeneous alloys, with refined grain structures, and long solid solubilities, resulting in a greater strength, hardness and thermal stability. The properties of aluminum alloys are further

enhanced by the addition of alloying elements, e.g. manganese and rare earth metals, which strengthening effects can be solid solution strengthening, precipitation hardening, and grain boundary pinning [3].

Aim

To Determine the influence of Ce and Y Additions and high energy ball milling treatment on the Microstructure and Mechanical Properties of the Al-Mn-Zr alloys to develop high-strength materials capable of performing at elevated temperatures.

Objectives:

1. Analyze the powder particles size, microhardness, phase composition, grain size of the aluminum based solid solution after milling.
2. Analyze the influence of annealing time and temperature on hardness, microhardness, and density of the hot-press sintered alloys.
3. Investigate the phase composition, grain size and hardness evolution in alloys sintered at 350 and 450 °C and further heat treatment.
4. Examine the effect of Ce and Y on the microstructure, mechanical properties and phase composition of Al-Mn-Zr alloys to determine the perspective alloys compositions and treatment.

LITERATURE REVIEW

Introduction to Aluminum alloys

Engineers often choose aluminum alloys since they are light, not easily corroded, and strong. These metals are split into wrought and cast alloys. Wrought alloys in the Al-Mn group are valued because they are both flexible and sturdy [4] Manganese (Mn) gives the alloys greater resistance to corrosion and strengthens solid solutions, while rare earth elements including lanthanum (La). Because cerium (Ce) and neodymium (Nd) make grain structure finer and improve thermal stability [5]. Aluminum-alloys are now more popular in industry. The good points about these materials are their strength compared to weight, simple processing, being flexible, excellent heat conduction, resisting rust, and a pleasant natural look. Aluminum alloys are flexible to use as they can be easily made into any shape, allowing for complex cross-sectional geometries. Certain important properties of aluminum alloys are functions of chemical composition, microstructure, and processing history. Their density is 2.7 g/cm³, which makes them light and useful in aerospace and automotive applications. They are also good in corrosion resistance dating back to their thin oxide layer which makes them useful in marine and chemical processing. Moreover, alloys that contain alloying elements such as copper, magnesium, and zinc are much stronger and hence used widely in aerospace structures [6].

Aluminum alloys are grouped into two broad categories; wrought alloys and cast alloys. This is represented in fig. 1 wherein the Aluminum alloys are classified with the wrought alloys further divided into heat-treatable and non-heat-treatable alloys, and the cast alloys being divided based on their main alloying agents.

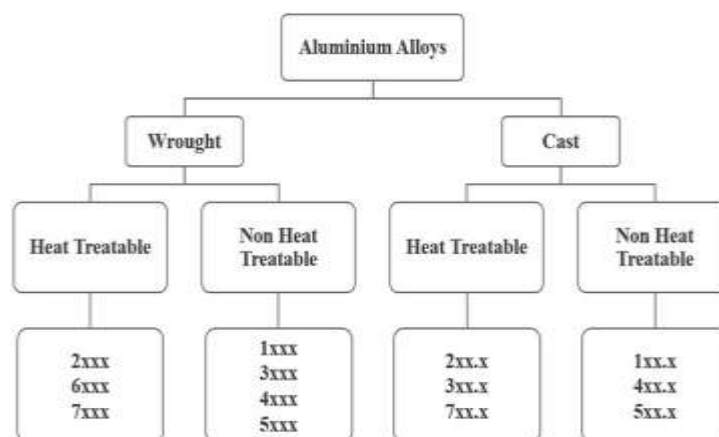


Figure 1 – Classification of aluminum alloys [7]

Wrought Alloys produced through mechanical working (rolling, extrusion, forging). Applications of these types of alloys normally involve areas that need high strength and ductility. The most important wrought alloys are the 1xxx series (pure aluminum), the 2xxx (Al-Cu), the 5xxx (Al-Mg), and 7xxx (Al-Zn) series. An extremely good example of which is the Al-Mn (3xxx) series where manganese is a major alloying addition, and which is widely utilized in beverage cans, and heat exchangers due to its good corrosion resistance, and formability [4].

Cast Alloys: Suitable for processes like sand casting, die casting and investment casting. They are usually used in applications where complex shapes and good machinability are needed. The 2xx are common cast alloys. 2xx.x (Al-Cu), 3xx.x (Al-Si-Cu), and 5xx.x (Al-Mg) series. Silicon (Si) is added to cast alloys to enhance their fluidity and decrease the solidification shrinkage, such properties make them suitable for automotive parts such as engine blocks and cylinder heads [8].

Recent advancements in technology, including additive manufacturing (3D printing) and direct metal laser sintering (DMLS), have greatly improved aluminum alloy properties and applications. These techniques enable the production of complex aluminum alloy components with custom microstructures and characteristics, making them especially useful in aerospace and automotive applications [9]. The process illustrated by Figure 2 begins with melting and fusing metal powders by using a laser or electron beam. It takes as inputs the standard Al7075 power feedstock and those that have been processed with nanoparticles. Nanoparticles encourage different and even grain growth, which lessens the weight of the strain from solidification. Using this method, alloys do not develop hot cracks and are designed in the best possible way.

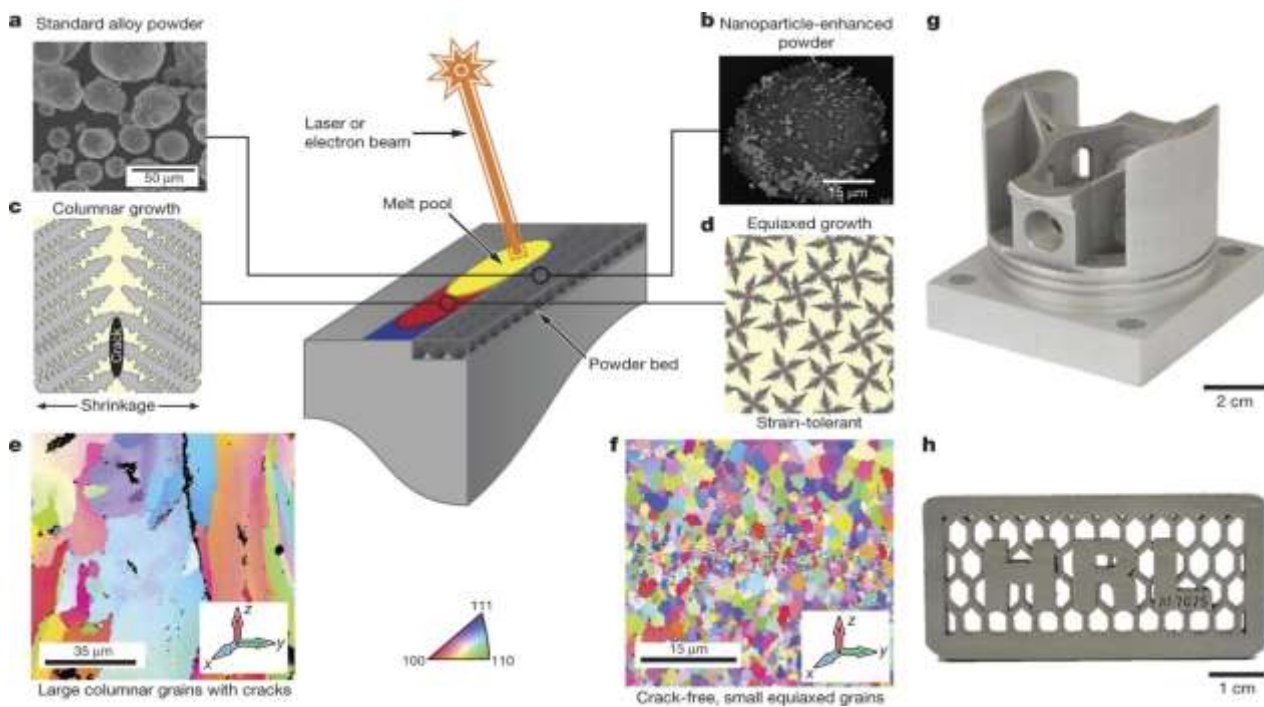


Figure 2 – Recent advancement in technology of aluminum alloys [10]

Nanostructured Aluminum Alloys: The creation of nanostructured aluminum alloys has resulted in considerable increases in strength, hardness, and thermal stability. These alloys are created by advanced processing techniques like severe plastic deformation (SPD) and mechanical alloying [9].

Recycling and Sustainability: Recent advances in recycling technology have enhanced the quality and characteristics of recycled aluminum alloys. Solid-state recycling and melt purification techniques have decreased contaminants in recycled aluminum and improved its mechanical characteristics. The advancement of high-temperature aluminum alloys with higher thermal stability and creep resistance has increased their use in the aerospace and automotive industries. These alloys are created by combining alloying elements like zirconium (Zr) and scandium (Sc), which generate stable precipitates at high temperatures [11].

Role and properties of Alloying Element

The addition of alloying materials significantly alters the properties of aluminum alloys.

Manganese (Mn)

Manganese is a key alloying element in the 3xxx series of alloys, increasing strength and corrosion resistance through the formation of tiny dispersoids during solidification. Additionally, Mn improves the work-hardening ability of aluminum alloys, making them ideal for high-ductility applications [12].

Copper (Cu)

Copper is the main alloying element in the 2xxx series alloys. It greatly boosts strength by forming precipitates like Al_2Cu during aging. However, Cu decreases corrosion resistance, limiting the use of these alloys in some situations [4].

Zirconium

Zirconium is a common additive to aluminum and alloys, with its solubleness in aluminum at 660 °C. Adding 0.02–0.2 wt.% increases strength by nearly three times and maintains properties up to 300 °C. It also enhances resistance to fatigue, corrosion, and natural aging [12] [13].

Zinc (Zn)

Zinc is the main alloying ingredient in the 7xxx series alloys. It produces precipitates like as $MgZn_2$ during the aging process, which considerably enhances strength. These alloys are commonly utilized in aeronautical applications due to their high strength-to-weight ratio [14].

Rare Earth (RE)

Rare earth Elements optimize grain structure, improve thermal stability, and improve mechanical qualities like hardness and tensile strength For example, [5] found that adding RE components to Al-Mn-Cu-Zr alloys resulted in a fine-grained microstructure with higher mechanical properties.

Yttrium

Yttrium, a rare earth (RE) element, improves thermal stability and oxidation resistance in aluminum alloys. [15] found that nanoscale Al_3Y precipitates restrict grain formation at high temperatures and improve creep resistance. Yttrium also improves microstructure by inhibiting recrystallization, making it suitable for high-temperature aerospace applications [16].

Cerium

Cerium is another RE element that greatly enhances mechanical strength and corrosion resistance in aluminum alloys. It produces Al-Ce intermetallic (e.g., $Al_{11}Ce_3$) that are thermally stable up to 300–400 °C, preventing over-aging [17] Ce also improves castability by lowering hot cracking and increasing fluidity, making it excellent for additive manufacturing of high-performance Al alloys [18].

Significance of High Alloyed Al-Mn-RE Alloys

High-alloyed Al-Mn-RE alloys have garnered significant attention due to their exceptional mechanical properties, corrosion resistance, and suitability for high-temperature applications. Figure 3 illustrates Application and significance of high alloyed Al alloys These alloys are widely used in aerospace, automotive, and structural engineering industries, where lightweight materials with high strength and durability are essential [4] [8].

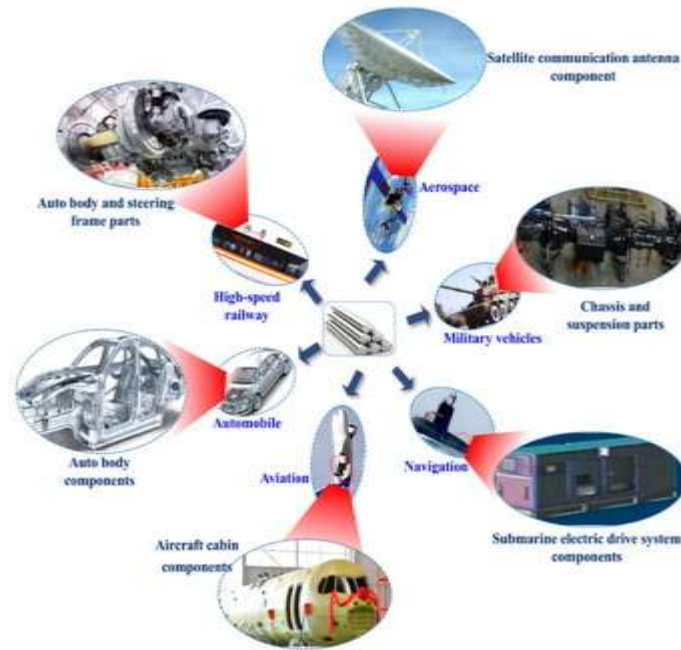


Figure 3 – Application and significance of high alloyed Al alloys [19]

The incorporation of RE elements into Al-Mn alloys has been shown to significantly improve mechanical properties, such as hardness, tensile strength, and fatigue resistance. For instance, [20] demonstrated that high-energy ball milling followed by hot-press sintering results in a fine-grained microstructure with enhanced mechanical properties. However, challenges remain in optimizing the alloy composition and processing parameters to achieve consistent performance in high-temperature environments [21].

Improved mechanical properties

Al-Mn alloys gain increased hardness, tensile strength and fatigue resistance when they are mixed with rare earth (RE) elements. Lanthanum (La), cerium (Ce) and neodymium (Nd) in REs are thought to produce a fine grain structure and bring about many fine precipitates which play a role in strengthening the alloy through precipitation hardening and strengthening the boundaries between grains [18] [17]. The presence of RE elements made these qualities reliable since they enhanced the formation of Al-RE and Al-Mn-RE phases.

By adding rare earths, zirconium alloys gain resistance to heat-related changes in structure, [11] according to [16],[17]. In aerospace and automotive areas, this quality becomes very important as materials must work in terrible weather conditions [18].

Microstructural Refinement

The addition of RE elements to Al-Mn alloys results in significant microstructural refinement, which contributes to their superior mechanical and thermal properties. RE elements promote the formation of fine, uniformly distributed precipitates and inhibit the growth of coarse intermetallic phases, leading to a homogeneous microstructure [9] Grain Refinement: RE elements act as grain refiners, reducing the grain size and improving the mechanical properties of the alloys. For example, [22] demonstrated that mechanical alloying of Al-Mn alloys with RE elements resulted in a fine-grained microstructure with enhanced hardness and tensile strength.

Mechanical Alloying

In mechanical alloying (MA), powder particles are repeatedly aggregate, fractured and welded to each other. Consequently, pure alloys are produced and their microstructures as well as personal characteristics become distinctive. It is especially helpful in producing advanced materials, such as, nanocrystalline alloys, amorphous alloys as well as metal matrix composites [24].

In the 1960s, Benjamin et al. came up with mechanical alloying to create oxide dispersion-strengthened (ODS) superalloys for applications at high temperatures. Over the years, MA has been applied to make different advanced materials, like aluminum alloys, titanium alloys and intermetallic compounds. MEA joins elements on a molecular or atomic level when subjecting them to ball milling with intensive energy. Apart from combining elements, this approach uses powders and ceramics which can be oxides or nitrides, to produce both alloys and composites. In 1966, at Inco's Paul D. Merica Research Laboratory, Benjamin and his coworkers first explored the approach [24]. The program tried to produce oxide-dispersion strengthened (ODS) superalloys made of nickel for use in gas turbines. Benjamin's team used a technique called ball milling to coat the oxide particles with nickel which served as their primary purpose in the beginning. Figure 4 illustrates the appearance of flatter surfaces, the formation of cracks and changes in particle size during mechanical alloying. These advantages have made MA a very useful tool for those working in materials science and engineering [24].

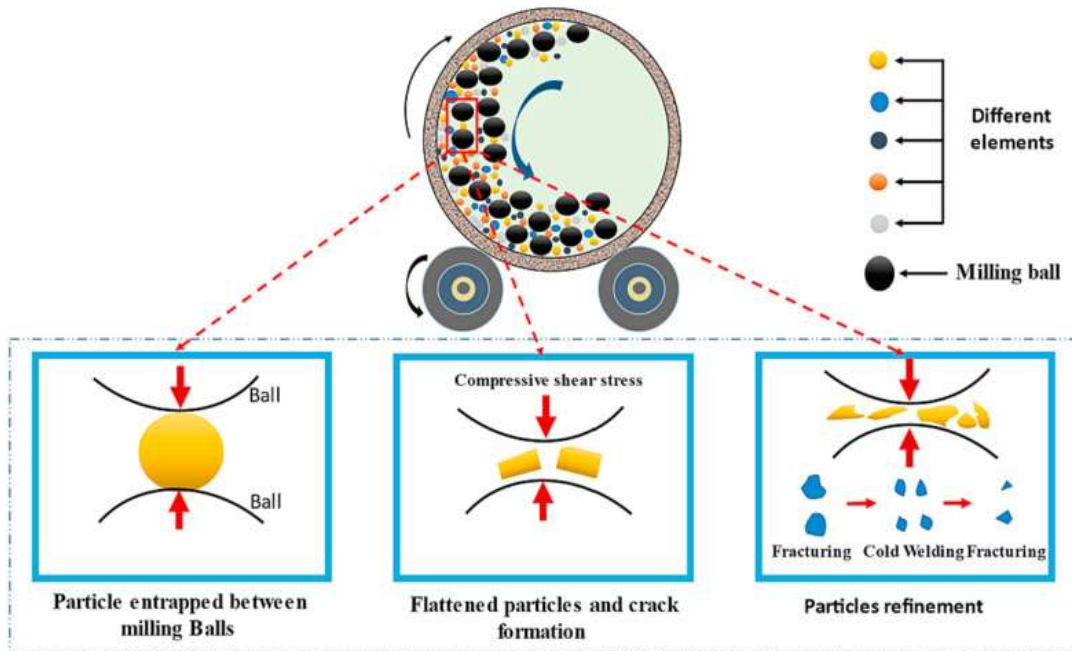


Figure 4 – Overview of mechanical alloying [25]

Mechanical Alloying Principles

The process of mechanical alloying involves repeatedly deforming, cold welding, and fracturing powder particles in a high-energy ball mill. Mechanical energy from the milling media (balls) transfers to the powder particles, resulting in atomic-level mixing and the formation of new phases [26].

Mechanisms for Mechanical Alloying

To begin the MA process, tiny particles are flattened and welded together to make multilayer composite particles. During the intermediate stage, composite particles are altered more and eventually begin to break which helps improve the microstructure and results in new phases. The last stage has the particles reach an equilibrium when they are all the same size and have the same mixing of alloys [24].

There is a disagreement among researchers since some argue that using MA on alloys such as aluminum and titanium is unsuitable because it may cause contamination and the appearance of unwanted intermetallic phases. Besides, due to high power usage and slow processing, it is hard to use MA for industrial apps [21]. Common choices for mechanical alloying/milling in material science are Spex 8000, planetary mills by Fritsch and Retsch, and Szegvari attritor. The energy is received by micro powder balls, either by shearing or by high-speed collisions with it. The first high-energy ball mill made for mechanical alloying was made by Benjamin, in the form of the attritor. In 1922, Szegvari came up with the attritor which soon improved how sulfur particles are distributed during rubber vulcanization. There is a cylindrical length added to the attritor and it holds all the powder and different-sized balls. Because of horizontal impellers on a vertical shaft, the balls and powder are easier to move and rotate [27], as seen in Figure 5.

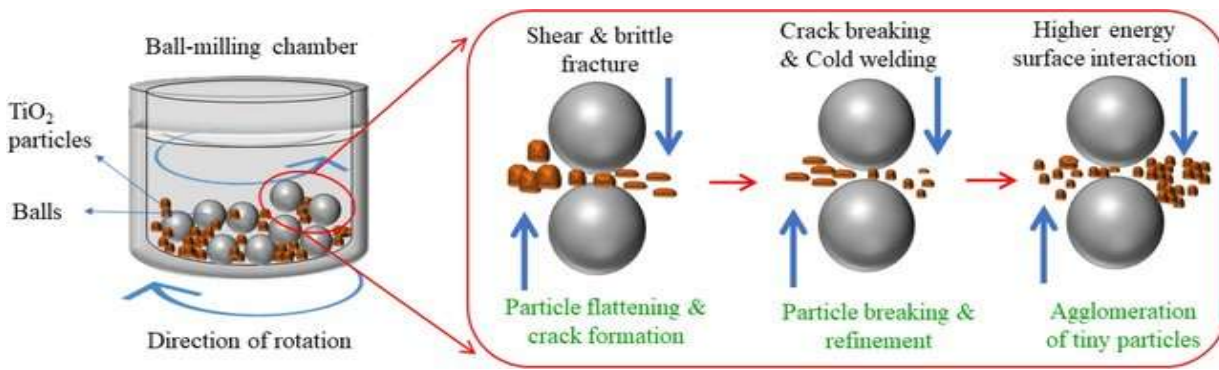


Figure 5 – High energy ball milling [27]

The impellers are organized in a progressive manner and perpendicular to one another. This design activates the balls, reducing powder size through impact. Because of their higher capacity. Attritor mills [27] are used for industrial purposes more than in research labs. Tumbler mills which are typical in mineral processing, can also be used for mechanical alloying (MA) as long as their diameters are large (on the meter scale) and they work in either the high energy impact mode or the low energy shear mode [28]. Unlike other mills, this one can modify the speed and frequency of impacts independently, keeping the machine's energy usage at the right level. Apart from the mills listed before, other options are available. There are situations where mechanical alloying is created by both rolling and ball mill processes [29].

Types of High-Energy Ball Milling mechanisms

The HEBM process incorporates a number of mechanisms, including: Head-on Impact: A direct impact between the milling ball with the powder particles. And Joining the Impact: Using numerous strikes to accomplish successful alloying. Multi-Ball Impact refers to the simultaneous collision of multiple milling balls with powder particles. These mechanisms are crucial to defining the efficiency and effectiveness of the milling process [24].

Head on impact

Such collisions make a significant impact on how the powder is structured. During an impact, the local compression leads to the production of small grains and evenly spread alloying elements. Impacting the milling ball directly against particles makes the materials stronger and harder [9]. With this collision, the big forces lead the powder to form distortions, connect and break in different parts. These frequent head-on collisions improve the microstructure and add new components to aluminum [26]. [9] looked at the effects of head-on impacts on the elimination of Mn and Al-Mn complexes in aluminum. The analysis indicated that continuous head-on impacts brought about a fine microstructure with uniformly spread precipitates which led to much better mechanical qualities in the alloy.

Joining the Impact

Combining numerous impacts boosts the impact and enables proper alloying. Steel made using this process involves repeatedly shaping, combining and breaking down the powder which results in fine microstructures of homogenous alloy [24]. The impact helps enhance the process of making steel by alloying. Because of many impacts, diffusion and the formation of new phases are enhanced in the material. After studying Al-Mn-Cu-Zr alloys mixed and processed this way, researchers found new improvements in material mechanical characteristics and thermal stability [9]. It was observed that mixing various impacts increased the alloy's uniformity, improved its microstructure and increased its mechanical properties.

multi-ball impact

Multi-ball impact is the simultaneous contact of many milling balls with powder particles. This type of collision causes significant local stresses, which promotes powder particle deformation, cold welding, and fracture. Repeated multi-ball impacts polish the microstructure and generate new phases [24]. Multiball impacts have a major impact on the microstructure of milled powders. Figure 6 shows the impact between the milling ball with

the powder particles of different mechanisms of mechanical alloying The high local stresses created by the impact encourage the production of fine grains and the homogeneous dispersion of alloying elements. This produces materials with higher mechanical qualities like hardness and tensile strength [9] Optimizing the milling parameters, such as ball-to-powder ratio, milling speed, and milling time, is critical for improving the efficiency and scalability of the high-energy ball milling process. Advanced modeling and simulation techniques can be used to predict the optimal milling parameters for specific alloy systems [24].

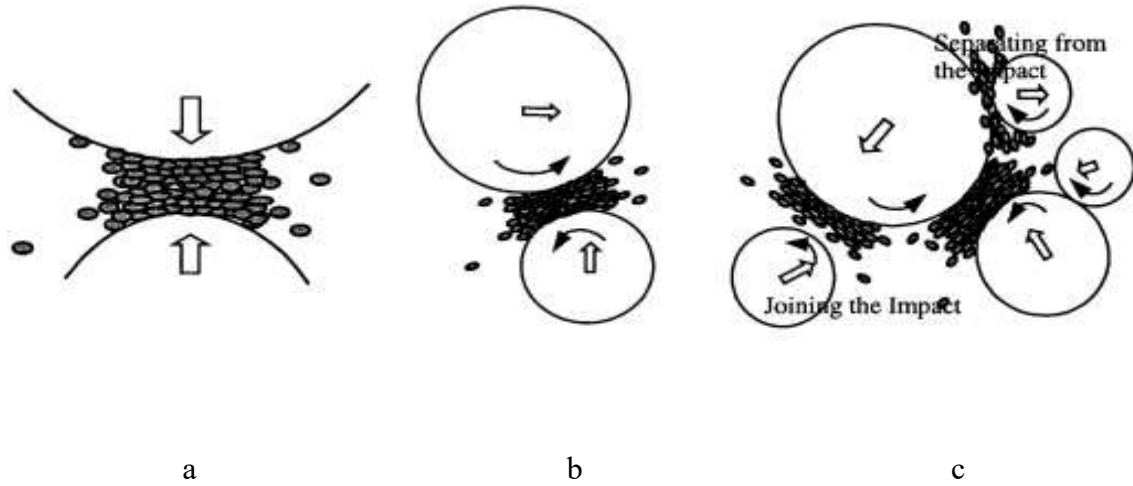


Figure 6 – Mechanisms of mechanical alloying (a) head on impact (b) joining the impact (c) multi ball impact [30]

Techniques of Mechanical Alloying

High-energy ball milling is the most common technique used for mechanical alloying. It involves the use of a high-energy ball mill, which generates intense mechanical forces through the collision of milling balls. The process parameters, such as ball-to-powder ratio, milling speed, and milling time, significantly influence the microstructure and properties of the final product [24].

High-energy ball milling (HEBM) is a mechanical alloying technique in which milling balls repeatedly collide with powder particles. As illustrated in Figure 7 below the technique is distinguished by a high energy input, which results in microstructure refinement, metastable phase development, and the synthesis of advanced materials including nanocrystalline alloys and metal matrix composites [24].

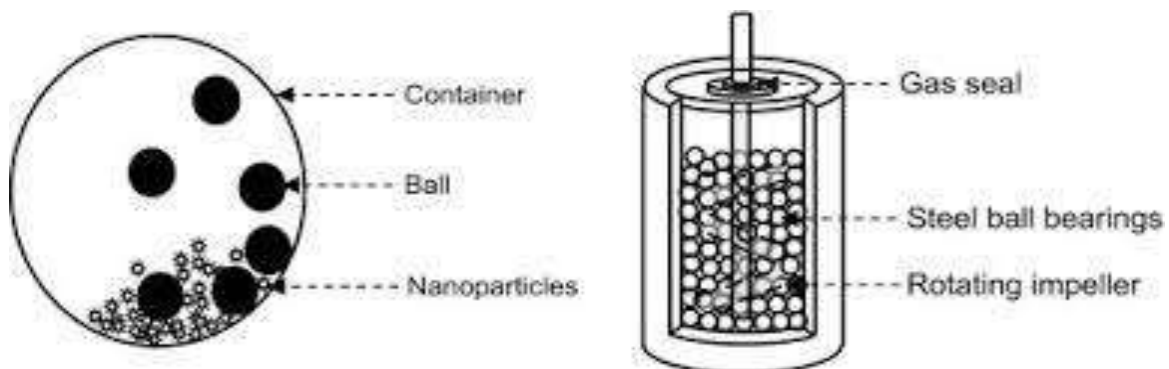


Figure 7 – High energy ball milling technique [24]

Planetary Ball Milling

Planetary ball milling is a type of high-energy ball milling that makes use of a planetary ball mill. Figure 8 illustrates different types of ball milling Planetary ball milling has a larger energy input and more uniform milling than traditional ball milling, making it suited for manufacturing nanocrystalline and amorphous alloys [9].

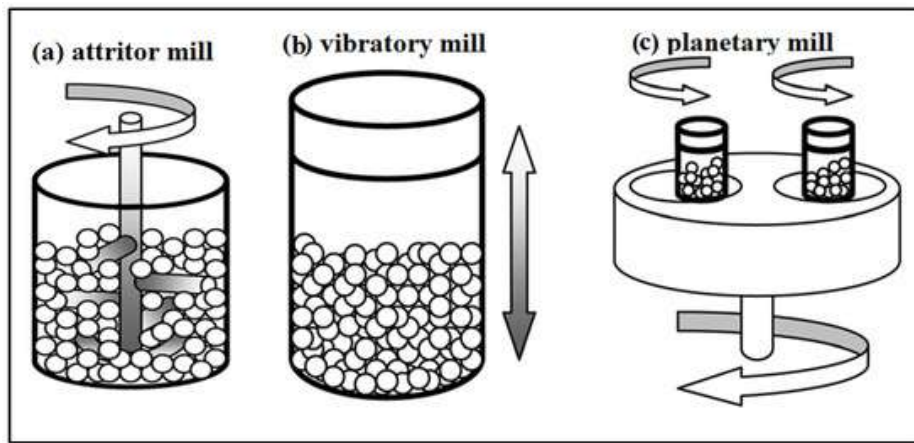


Figure 8 – Types of ball milling [31]

Attrition milling

Attrition milling is another way of mechanical alloying. It makes use of a spinning drum filled with milling balls and powder particles. The technology offers little energy input and longer milling durations, making it suitable for creating fine powders with controlled particle size distributions [24].

Mechanical Alloying Process

Powder Preparation

The MA process begins with the preparation of the powder mixture. The powder particles are typically blended in a predetermined ratio to achieve the desired alloy composition. The use of high-purity powders is essential to minimize contamination and ensure the formation of homogeneous alloys [26].

Milling Parameters

The way the mill is set up, for example, ball-to-powder ratio, milling speed and milling time, is essential for the final looks and quality of the product. If the ball-to-powder ratio is large and the milling speed is high, the alloying process may be accelerated, but this could also cause a lot of impurities and clusters. Having a large portion of powder can help go through the metal faster, however, it may increase the chance for contamination and clumping of particles. If there is not enough powder compared to the amount of ball in a mix, the aluminum alloy may not be completely formed and it could contain uneven microstructures [24]. Faster milling speeds contribute to a rise in the energy needed and increase the speed of combination between base materials and alloying elements. Elevated milling speed increases the speed of the alloying process; however, it may also cause the part to get too hot and be contaminated. Conversely, when the milling speed is slow, not all the alloying occurs and the structure is not uniform.

How long the milling process runs is also very important. Milling for a long period can cause parts of the product to become both nanocrystalline and amorphous, though it can easily lead to contamination and the formation of larger particles. If milling does not last long enough, the alloying may be imperfect and the structure inhomogeneous [24].

Milling balls give energy to the powder which changes the handling of alloying and other phase changes in MA/MM. Many factors play a part in the process of energy transfer, for instance, the mill's special features, how fast milling happens, the size and type of balls, the amount of powder versus balls, how full the vial is, if grinding is done in water or air, the temperature during grinding, the air and temperature inside the mill and the time spent milling. Using faster milling speeds or heavier balls leads to a rise in the kinetic energy of the balls and tungsten carbide stones show the best results among them. It has been found by several researchers [32]. [33] that a faster milling process can actually widen the range of materials known as glass formers. [34] found that the level of NiAl produced and its tendency toward disordering go up as the MA process becomes more

intense. Other studies found out that the speed of titanium carbide (TiC) formation during mechanical alloying (MA) increases by a large amount with each tiny adjustment in milling ball density [35].

The choice of ball size, the way balls are dispersed and their overall number should help achieve the most efficient usage of the vial. A big collection of balls close together reduces the distance between collisions, though looser packing reduces how often the balls hit. It is common to use ball/powder weight ratios from 5:1 to 10:1 and the results suggest they work very well.

In high energy ball milling, powder grains tend to vibrate together and generate cracks. How strongly and where the material fractures is affected by its ability to deform and the temperature at which it is milled. This means that the milling process's major phase transition events are mainly affected by the temperature used in milling. [36] studied the effects of combining silver and copper into an alloy. Mixing the systems together gives off heat. It was found through the study that solid solutions stay intact at low milling temperatures, but higher temperatures lead to their breakdown. While the balls are rotating during milling, some of their energy turns into heat which makes the powder get warmer.

In MA, powder particles are welded together and then fractured repeatedly while colliding inside the balls in a mill. How strong or tough the powder particles are greatly affect's the actions that happen during welding and when the material breaks. Consequently,

Ductile/ductile systems

Many alloyed elemental mixes belong in this group, since is the first to describe the process. . [37] Later, Benjamin wrote additional papers to give a deeper analysis of this subject. Through optical microscopy, the MA process can be simply divided into five parts which these results confirm. Figure 9 illustrates What happens when a ball collides with powder.

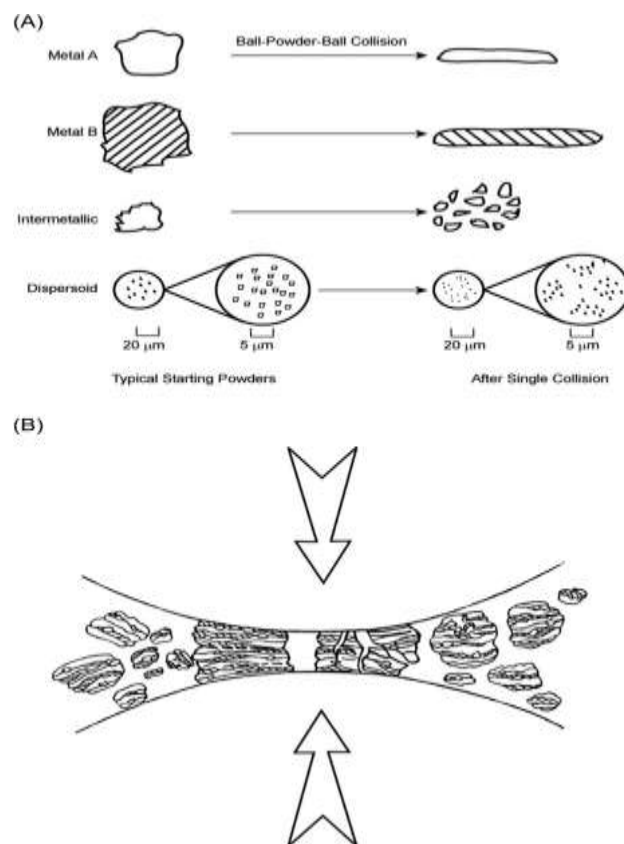


Figure 9 – Events that occur during the ball-to-powder impact [25]

This figure demonstrates the way the powder particles get trapped among two balls impacting each other. From the beginning, micro forging deforms equiaxed ductile particles into a flat and flaky form. Milling at lower temperatures causes a sandwich-like structure and also makes the particle size larger. The third stage of the

process. Fracturing may occur more often in this step as strain hardening makes particles tougher and more likely to break. During random welding orientation, several groups of lamellar colonies are created inside the particle and these groups have no fixed orientation. When equilibrium is reached, the material's hardness and particle size end up at their maximum values which means there is balance in how fast the material welds together and breaks down. After five cycles of mechanical alloying (MA), lamellar structures in the particles are so small that they become invisible under an optical microscope. In alloying, the initial phase is diffusion which happens during or at the final phase of the third stage. It is possible because carbon and silicon develop fine repeating bands made up of each element. Furthermore, milling at elevated temperatures and having defects caused by deformation makes it easier for alloying elements to move in the material. During the fifth step of the MA process, the alloying procedure is achieved. Examples of ductile/ductile systems are Ni-Cr, Cu-Ni, Cu-Zn and Ni-Al. Choosing a stoichiometric mix resulted in synthesizing Nb₃Sn [38], a superconducting compound, owing to the addition of MA of Nb and Sn in this categorization. Making Mn Bi through mechanical alloying of manganese (Mn) and bismuth (Bi) is another way that falls into this group as well [39].

Ductile/brittle systems

In the beginning, Benjamin and his group proved that some ODS alloys were ductile/brittle with their research. Oxide particles are spread evenly along with the ductile phase, while the separate layers of the steel join together.[40].

Brittle/brittle systems.

At the beginning, experts thought that brittle-to-brittle milling would result in the particles breaking and no alloying would happen. In fact, it is clear that the alloying process works well with the Si-Ge system using powder milling [40]. A number of NiZr₂ and Ni₁₁Zr₉ intermetallic compounds were milled to produce amorphous alloys [40], [41]. These cases demonstrate that using alloys and transferring materials is possible during high energy ball milling of brittle/brittle materials. Even so, there is a lack of clear knowledge about how these alloying mechanisms work. Granular systems that underwent mechanical alloying were found to display microstructure characteristics that set them apart from lamellar types, mainly those that behave in a ductile way. It is believed that the transfer of material happens because of diffusion during the temperature rise that happens during milling.

Morphological evolution during mechanical alloying

The impact of mechanical alloying on ductile powders was explored [40] [42] . It was found in their investigation that the process involves some key steps, as presented in Figure 10. At first, it is important to mix and fuse the powder particles. First, deformation and welding resulted in flake particles with layers of alloy materials mixed together. While powder particles are being welded, the number of particles reduces as the size of the particles increases. In addition, subjecting the particles to mechanical alloying caused a lot of plastic deformation which made their hardness increase a lot.

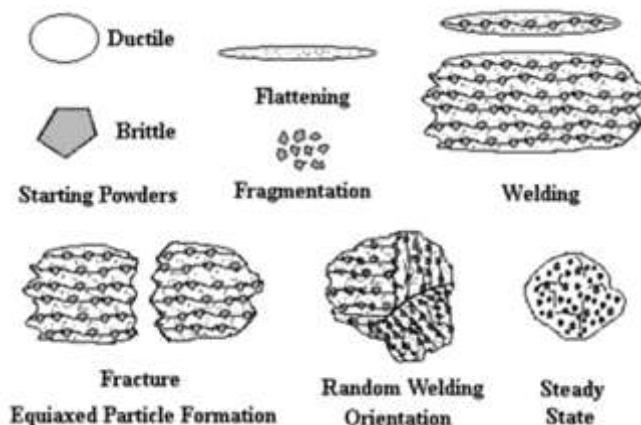


Figure 11 –. The different stages of mechanical alloying in ductile-brittle system [46]

the process. A model was proposed [43] [44] [45] after researching the stages of particle. Afterward, fine-grained particles called equiaxed started to form and the clumping of layered particles resulted in irregular particle direction. At the same time, particle size is less which forms a complex pattern like marble. Because particles are getting harder and less ductile, there is a higher probability that they will break. However, it is during the last step of mechanical alloying that each particle arrives at the overall composition and hardness. Besides the aforementioned reasons, 37 equilibrium maintains the fracture-welding process at a steady level which ensures the mean particle size is almost unchanged at the very end of formation by milling and this model described A and B type particles coming together.

Relevant Investigations on Mechanical Alloying for Aluminum Alloys

The study [15] looked at how Al-Mn-Cu-Zr alloys were formed and what characteristics they possessed as a result of mechanical alloying. It was found in the study that ball milling at high power and then sintering with heat led to a finer microstructure and enhanced hardness and tensile strength. Thanks to the RE elements, these alloys formed strong intermetallic complexes which raised their strengths. [15] They found that including Zr into the alloy increased its hardness and tensile strength. As the aluminum alloys aged, small particles known as precipitates formed and made the properties listed above even better. Sc and Zr in the alloys raised the alloys' ability to stand up to temperatures and avoid softening, making them fit for high-temperature processes.

Hot press sintering (HPS)

HPS stands for hot press sintering and it helps produce solid and robust materials. It is a great way to consolidate mechanically alloyed powder thanks to the refined grains and smaller numbers of pores it brings. In Figure 11, the hot press sintering process is clearly presented and it is majorly applied to create sophisticated materials such as aluminum alloys, titanium alloys and metal matrix composites [47] [48].

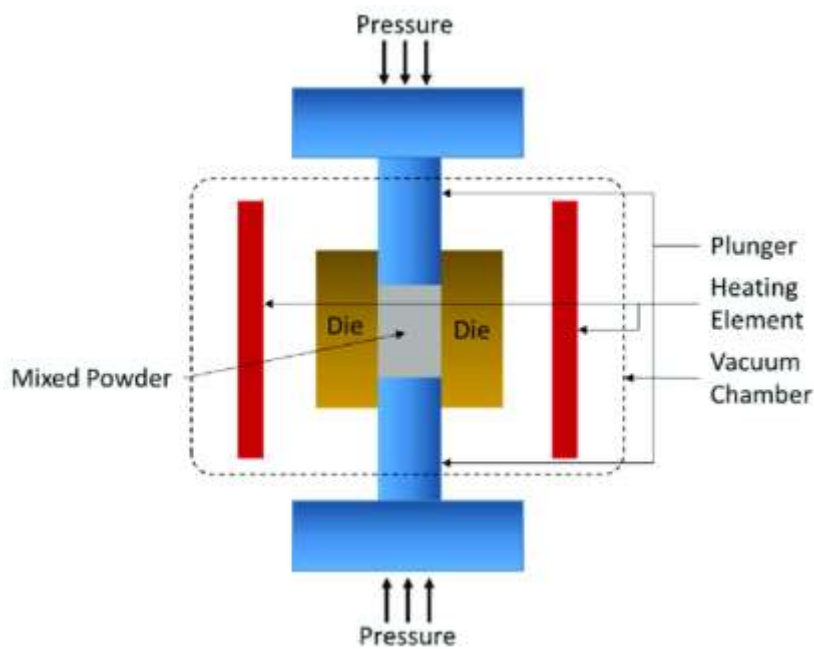


Figure 11 – Schematic setup for hot press sintering [49]

Historical Development

In the early 20th century, hot press sintering was developed to produce dense ceramic materials. Since then, it has been adapted to produce metallic materials with complex compositions and microstructures. Advancements in sintering equipment and process control systems have expanded HPS's applications in materials science and engineering [47] Hot Press Sintering (HPS) is a valuable tool for producing advanced materials with high density, fine grain size, and superior mechanical properties. It is especially useful in high-temperature and high-stress applications [48].

Process Parameters of Hot Press Sintering

The sintering temperature plays an essential role in HPS due to its impact on densification and microstructure of the final product. At high sintering temperatures, atoms diffuse and make strong interparticle bonding, leading to a high-density product. Nevertheless, high sintering temperatures may cause a grain coarsening and mechanical properties deterioration [47].

The sintering pressure is another critical parameter in HPS, as it influences the mechanical properties of the end product. High sintering pressures promote the consolidation of powder particles and the formation of dense, high-strength materials. However, excessive sintering pressures can lead to cracking and deformation, particularly in materials with complex shapes [48].

The holding time refers to how long the material remains at the sintering temperature and pressure. The holding period affects the degree of densification and the development of interparticle connections. [47] The heating rate is the pace at which the material reaches the sintering temperature. The heating rate effects the final product's microstructure and characteristics. High heating rates can cause thermal gradients and uneven densification, whilst low heating rates can result in excessive grain growth [48].

Impact of Hot Press Sintering on Al-Mn-RE Alloys

Hot press sintering promotes the refinement of the microstructure in Al-Mn-RE alloys, resulting in fine grain size and uniform distribution of precipitates. [50] The mechanical properties of Al-Mn-RE alloys are significantly influenced by the HPS process parameters. High sintering temperatures and pressures promote the formation of strong interparticle bonds and fine-grained microstructures, resulting in materials with superior mechanical properties. However, excessive sintering temperatures and pressures can lead to grain coarsening and degradation of mechanical properties [50].

The thermal stability of Al-Mn-RE alloys is enhanced by the HPS process, as the fine-grained microstructure and uniform distribution of precipitates inhibit grain growth and recrystallization at elevated temperatures. This makes HPS-processed Al-Mn-RE alloys suitable for high-temperature applications, such as aerospace components and automotive engine parts [50].

Mechanical alloying is carried out under heavy plastic deformation of powder particles.[51] provided TEM evidence to be this hypothesis, in their study, showing the existence of shear bands due to the formation of non-uniform deformation induced during high-energy ball milling. Again, a research team carried out a study that confirmed that extreme plastic work can cause isolated phases within several Nanocrystalline alloys [46] [52] [53].

Grain boundary strengthening

It was found in 1950s by Hall and Petch that steel gets stronger when the grain size gets smaller. Working on their essential dislocation theory, they introduced the Hall-Petch connection related to dislocations building up next to each other. Still, this model may not be appropriate for grain sizes that are less than 100 nm. The Hall-Petch coefficient is not constant; sometimes, certain nanocrystalline alloys show lower yield strength thanks to the inverse Hall effect.[55] [56].

Solid solution strengthening

Adding more solutes amounts to concentrating the solution. That aside, there is general agreement that the addition of MA tremendously increases the ability of solids to dissolve. Therefore, the strength of MA alloys is expected to undergo a significant upgrade. Researching on nanocrystalline Al-Mn alloy [57].

Precipitate Analysis in Al-Mn-RE Alloys

Introduction to Precipitate Analysis in Al-Mn-RE Alloys Precipitate analysis is a critical aspect of materials science, particularly in the study of aluminum alloys. Precipitates are secondary phases that form during the

solidification or heat treatment of alloys, and they play a significant role in determining the mechanical properties, thermal stability, and corrosion resistance of the material. In Al-Mn-RE (aluminum-manganese-rare earth) alloys, precipitates such as Al-Mn, Al-RE, and Al-Mn-RE intermetallic compounds are key to enhancing strength, hardness, and high-temperature performance [58].

Precipitates in Al-Mn-RE alloys contribute to strengthening mechanisms such as precipitation hardening, grain boundary strengthening, and dispersion strengthening. The formation of fine, uniformly distributed precipitates during aging or sintering significantly improves the mechanical properties of the alloy, including hardness, tensile strength, and fatigue resistance) [50].

Rare earth elements such as lanthanum (La), cerium (Ce), and neodymium (Nd) are known to refine the microstructure of aluminum alloys and promote the formation of stable precipitates. [59]. Manganese is a key alloying element in Al-Mn-RE alloys, as it forms stable intermetallic compounds such as Al₆Mn and Al₁₂Mn. These precipitates contribute to strengthening mechanisms and improve the thermal stability of the alloy [12].

Rare earth elements promote the formation of fine, thermally stable precipitates such as Al-RE and Al-Mn-RE compounds. These precipitates inhibit grain growth and recrystallization, enhancing the mechanical properties and thermal stability of the alloy [60].

Annealing in Al-Mn-RE Alloys

Annealing is a heat process whereby a metal is heated to a specific temperature and allowed to cool slowly. This softens the metal which means it can be cut and shaped more easily [60]. Mechanical properties (hardness, microhardness, and density) of Al-Mn-RE alloys are optimized due to annealing. The mechanism is beneficial to generate fine, homogeneously distributed precipitates, which can strengthen the precipitation hardening and grain boundary strengthening mechanisms [50].

Microstructure of Al-Mn-Zr-RE Alloys

The grain refining effect of Al-Mn alloys can be further enhanced by Zr, Ce and Y addition, and the refinement of grains was obtained in finer and superior mechanical properties were achieved., the fine grains inhibit the motion of dislocations and improve the alloying strength and hardness [50]. At elevated temperatures, these precipitates act as obstacles to the motion of the dislocations, resulting in grain refinement [11]. The phase transformation in Al-Mn-Zr-Ce-Y alloys is controlled by the alloy composition and heat treatment processes. It can be seen that the addition of Zr, Ce, and Y strengthens the formation of the stable intermetallic compounds improving the thermal and mechanical properties of the alloy [23].

Al-Mn-Zr-Ce-Y alloys' hardness and tensile strength are greatly increased by the production of fine grains and uniformly dispersed precipitates. For example, [50] found that high-energy ball milling followed by hot-press sintering produced a fine-grained microstructure with high hardness and tensile strength. The homogeneous distribution of precipitates in Al-Mn-Zr-Ce-Y alloys enhances fatigue resistance by preventing crack formation and propagation. This makes the alloys appropriate for cyclic loading applications such as aerospace components and automobile engine parts [16]. and the inclusion of Zr, Ce, and Y increases creep resistance in Al-Mn alloys by generating thermally stable precipitates that prevent grain development and dislocation motion at high temperatures. This makes the alloys appropriate for high-temperature applications like jet engines and exhaust systems [11].

METHODOLOGY

This study focused on the process flow of the Al-Mn-Zr-RE alloys, including initial alloy melting and casting, mechanical alloying, and compaction by hot press sintering, followed by characterization. Its approach was to obtain a homogeneous distribution of alloying elements by controlling microstructure and phase stability and demanding mechanical stability at high temperatures. The rare earth (RE) elements used, which are zirconium (Zr), yttrium (Y), and cerium (Ce) were selected based on their established abilities to refine microstructure, increase recrystallization resistance, and stabilize thermally favorable phases [4].

Materials

Raw Materials

The starting materials used are the Al-10 wt%Mn, Al-20 wt% Ce, Al-9wt%Y master alloys and commercially pure Zr (99,9%). As illustrated in the Table 1 below.

Table 1 – The composition of the studied alloys, at. %

Sample	Mn	Zr	Y	Ce
Al-Mn-Zr	4.0	1.2	–	–
Al-Mn-Zr-Y	4.0	1.2	0.6	–
Al-Mn-Zr-Ce	4.0	1.2	–	0.6

Mechanical Alloying Process

Shear-induced solid-state reactions at small deformations during mechanical alloying (MA) are an integral part of this work with the objectives being to control microstructure, homogeneously segregate RE elements, and stimulate the formation of a hardening phase of interest. The master alloys and Zr were crushed and ground into chips prior to mechanical alloying.

Selection of Mechanical Alloying Equipment

Planetary Ball Mill

Because of its high energy impact mechanism and excellent efficiency for homogenous mixing and alloying a planetary ball mill was selected. Such jars can rotate both on their own axes and around the common axis, which promotes effective energy transfer upon collision, allowing effective powder particles repeat fracturing and cold welding.

Milling Chamber with Balls

Stainless steel jars were selected for their durability and compatibility. Hardened steel balls (10 mm diameter) were used to maximize energy transfer. Airtight jars with a capacity of 500 ml provide an inert argon atmosphere for milling. The following parameters were adopted after preliminary testing and literature benchmarking [61] Milling speed: 300 rpm. The Ball-to-Powder Ratio (BPR) is 20:1 by weight, optimized for fine, homogeneous powders without excessive cold welding. Milling time is 20 hours, with cooling breaks every 2 hours to avoid overheating. To prevent powder agglomeration and cold welding, use ~1 wt.% stearic acid as a process control agent. Milling was carried out under high-purity argon to prevent oxidation.

Temperature Monitoring

A thermocouple incorporated in the milling chamber enabled real-time temperature monitoring. Milling temperatures were controlled below 70 °C using intermittent milling and active air cooling. To prevent oxidation, the powders were collected in an argon-filled glove box. The powder had a delicate, flaky morphology that is typical of ductile metal alloys subjected to MA.

The Hot Press Sintering Process

After mechanical alloying, the powder samples were compressed using hot press sintering (HPS) to form dense billets.

Equipment Used

The hydraulic hot press features a heating chamber and a vacuum/inert gas system. The die set has a 20 mm inner diameter and is lined with graphite foil to prevent powder adhesion. Thermocouples near the sample allow for precise temperature monitoring.

Sintering Conditions

Two sintering temperatures, 350 °C and 450 °C, were employed. Holding times of 15 minutes, 30 minutes, 1 hour, and 2 hours were examined. Uniaxial pressure of 50 MPa was applied during the holding step. High-purity argon gas was continuously flushed into the chamber. The sintered compacts were then cooled in the same controlled environment to room temperature before being extracted for analysis.

Characterization of Al-Mn-Zr-RE. Alloys

The sintered samples were thoroughly characterized to determine their microstructure, phase composition, thermal stability, and mechanical properties. The techniques used are scanning electron microscopy (SEM), X-ray diffraction (XRD), Vickers microhardness testing, and density analysis. Scanning Electron Microscopy (SEM) was utilized to analyze the morphology, grain boundaries, and distribution of intermetallic particles in sintered alloys. Preparation: Samples were sectioned, mounted, polished with diamond paste (to 0.05 μm), and etched with Keller's reagent (2 mL HF, 3 mL HCl, 5 mL HNO₃, 190 mL H₂O). Observation Mode: High vacuum with 15-20 kV of accelerating voltage. Magnification ranges from 500x to 10,000x for detailed microstructural analysis. Image analysis software was used to assess particle size distribution and grain refinement with RE additions. The presence of polished grains and uniformly distributed precipitates suggested increased heat stability and dispersion strength.

Phase Composition Analysis Using X-Ray Diffraction (XRD)

XRD was used to detect crystalline phases and assess lattice parameter changes caused by mechanical alloying and sintering. Instrument: PANalytical X'Pert PRO X-ray diffractometer. • Radiation source is Cu-Kα (λ = 1.5406 Å). • Scanning range is 20° to 90° 2θ. • Step size: 0.02°, scanning rate: 1°/min. The HighScore Plus software identifies phases using the ICDD PDF-4+ database. XRD patterns revealed the presence of primary Al matrix and intermetallic phases such as Al₁₁Mn₄, Al₃Zr, Al₈Ce, and Al₃Y. Peak broadening and shifts were also used to determine crystallite sizes and lattice strains, consistent with Williamson-Hall analysis [24].

Hardness tests

Microhardness tests were used to quantify the mechanical strength gains from alloying and annealing procedures. Instrument: LECO LM247AT microhardness tester. Test load is 100 g (HV0.1). Figure 12 illustrates hardness tester machines in MISIS laboratory Dwell time: 15 seconds. Measurements: Averaged five readings per sample. Sample conditions: Measurements were obtained before annealing and after heat treatments of 15 minutes, 30 minutes, 1 hour, and 2 hours at 350°C and 450°C. The hardness values increased significantly as the annealing time and temperature increased. At 450 °C for 2 hours, the Al-Mn-Zr alloy achieved the maximum microhardness (440 HV) due to Al₃Zr precipitation and grain refining.



Figure 12 – Microhardness tester in MISIS laboratory

Density Measurements.

The Archimedes' principle was utilized to determine the density of sintered samples. Medium: distilled water was used.

Statistical Analysis and Error Considerations

To confirm that the results were reproducible and reliable, all measurements were repeated several times under identical conditions. Microhardness testing was conducted at five sites for each sample. The mean and standard deviation were reported. Outliers exceeding $\pm 10\%$ were deleted. • Archimedes' density tests were done three times for each sample. Variability was $\pm 0.01 \text{ g/cm}^3$. Cross-validation of peak intensities and positions was performed using conventional PDF cards during phase analysis. Errors in peak broadening measurements were assessed based on instrument resolution, and data were adjusted using a silicon reference.

Data Processing Tools

Microsoft Excel, OriginPro 2023, and Minitab were used for data plotting, statistical treatment, and regression modeling where applicable.

ANOVA (Analysis of Variance) was applied to compare the effects of annealing time and temperature on hardness and density values. A p-value < 0.05 was considered statistically significant.

Waste Disposal

Metal waste and unused powders were collected in designated recycling bins.

Chemical wastes, such as spent stearic acid, were disposed of in accordance with institutional and environmental requirements.

Safety and Environmental Considerations

All synthesis and characterization operations followed safety and environmental protocols. Powders were handled in a fume hood to prevent inhalation risks. Always we wear nitrile gloves and anti-static lab coats. We Store stearic acid in sealed containers due to its flammability in powdered form. Argon was utilized for melting, mechanical alloying, and sintering to reduce oxidation and fire dangers.

Pressure valves, leak detection systems, and flow regulators ensured safe handling of gas cylinders. Furnace and Hot-Pressing Safety Operators adhered to thermal PPE requirements, including insulated gloves and face shields. • Emergency power cutoff and fire suppression systems were installed near furnace areas. Waste Disposal Metal waste and unused powders were collected in designated recycling bins. And Chemical wastes, such as spent stearic acid, were disposed of in accordance with institutional and environmental requirements.

Methodological Workflow Summary

The entire experimental methodology is summarized in Figure 13 in the flowchart below illustrating each key stage in sequence:



Figure 13 – Methodological summary

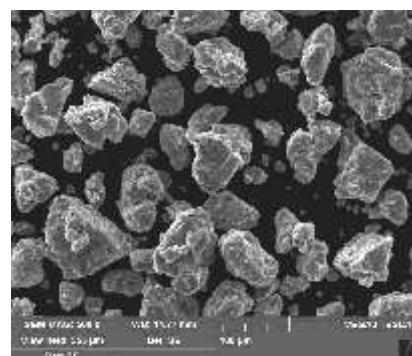
RESULTS AND DISCUSSION

3.1 Powder Particles Analysis

Figure 14 shows granular morphology of the alloys from SEM and TEM the powders showed a uniform particle size distribution.



a



b

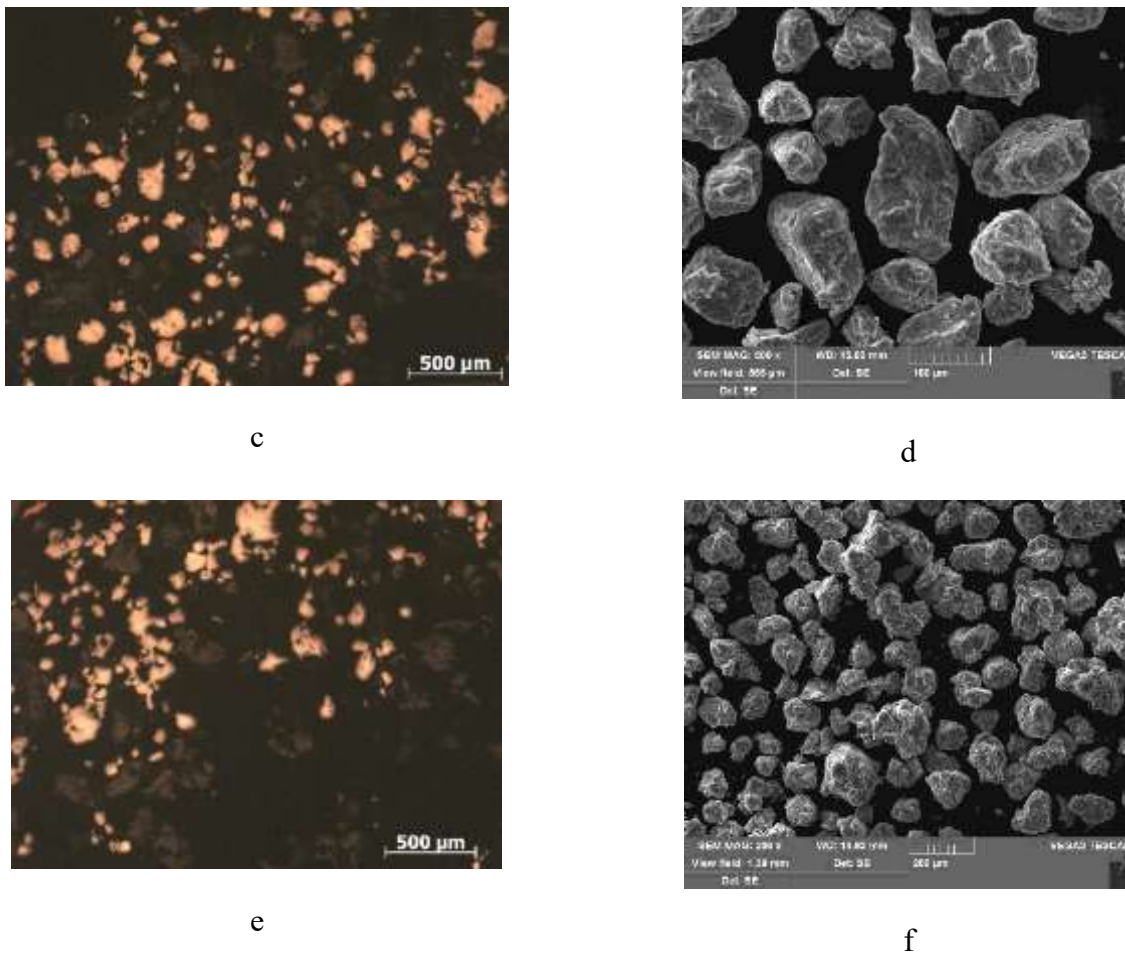


Figure 14 – Granular morphology of of (a) Al-Mn-Zr from TEM (b) Al-Mn-Zr from SEM (c) Al-Mn-Zr-Y from TEM (d) Al-Mn-Zr-Y from SEM (e) Al-Mn-Zr-Ce from TEM and (f) Al-Mn-Zr-Ce

Initially, large and irregular particles were observed, but they progressively became refined due to repeated fracturing and welding. By 10 hours of milling, the morphology was flake-like for Al-Mn-Zr and more equiaxed for Al-Mn-Zr-Y and Al-Mn-Zr-Ce, which indicates better powder flowability and compact ability for the RE-doped alloys. Based on what is shown in Figure 15, the number of small granules increased over time, proving the process of fragmentation during mechanical alloying.

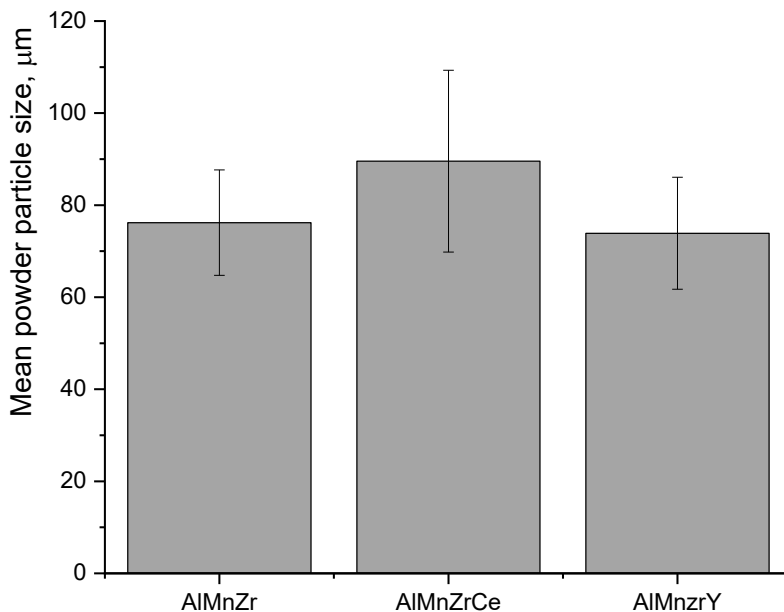


Figure 15 – Powder particle size for the alloys studied

X-ray diffraction (XRD) analysis

X-ray diffraction (XRD) was employed to analyze the crystalline phases present in the milled for 10 hours and compacted samples revealed distinct structural evolutions induced by the addition of rare earth elements (Ce and Y). Crystallite sizes calculated using the W-H equation indicate that the presence of RE elements influenced grain refinement, with smaller grain sizes generally correlating to higher peak broadening the lattice parameters varied widely between the three compositions. The lattice parameters were calculated assuming 100% solubility of each alloying element as determined using Vegard's law. The analysis of the crystallite size and lattice parameter indicated that there were remarkable differences between the Al-4Mn-1,2Zr base alloy and its Ce- and Y-modified variants, especially between various processing conditions. The grain sizes of milled samples were constantly the smallest, and the Al-4Mn-1,2Zr-0.5Y alloy had the smallest crystallite size (~16 nm), followed by Al-4Mn-1,2Zr-0,6Ce (~18nm) and Al-4Mn-1,2Zr (~20nm). Compaction produced a large grain growth, particularly at 450°C where crystallite sizes of up to ~84 nm in Ce- and ~81 nm in Y-containing alloys were achieved. This increase is indicative of thermal recovery and recrystallization processes which occur because of the high temperature of compaction. Conversely, the samples compacted at 350°C proved to have smaller grains indicating low atomic mobility.

There were also variations in lattice parameters. Phase stability was confirmed by the fact that most compacted samples (including those containing Y) were very near the FCC Al value (0.404 nm). There are however some anomalies including higher lattice parameters in Al-4Mn-1,2Zr compacted at 450°C (0.54 nm) and Al-4Mn-1,2Zr-0,6Ce compacted at 350°C (0.50 nm) which indicate possibility of internal strain or solute segregation. Conversely, the Y-modified alloy showed no variation in the lattice parameters in all the states (~0.4045–0.4047 nm), suggesting a higher solute solubility or less distortion.

These results affirm that milling causes extensive grain refinement, whereas thermal compaction, particularly at 450 °C causes grain coarsening, with Ce and Y having different effects on the magnitude of crystallite growth and lattice stability. This microstructure-thermal processing balance is important to maximize the mechanical properties in these enhanced aluminum alloys. The results are shown in Table 2 below.

Table 2 – Crystallite size and lattice parameters for the alloys-studied

Alloy	Crystallite size, nm	a_{avg} , nm	a_T (theoretical)
Al-4Mn-1,2Zr milled	20 ± 2	0.4039 ± 0.0001	0.4045
Al-4Mn-1,2Zr compacted 350	25 ± 8	0.4047 ± 0.0001	–
Al-4Mn-1,2Zr compacted 450	59 ± 7	0.4054 ± 0.0001	–
Al-4Mn-1,2Zr-0,6Ce milled	18 ± 4	0.4041 ± 0.0001	0.4046
Al-4Mn-1,2Zr-0,6Ce compacted 350	40 ± 9	0.4050 ± 0.0001	–
Al-4Mn-1,2Zr-0,6Ce compacted 450	84 ± 7	0.4051 ± 0.0001	–
Al-4Mn-1,2Zr-0.5Y milled	16 ± 2	0.4036 ± 0.0001	0.4041
Al-4Mn-1,2Zr-0.5Y compacted 350	46 ± 5	0.4045 ± 0.0001	–
Al-4Mn-1,2Zr-0.5Y compacted 450	81 ± 10	0.4047 ± 0.0001	–

The XRD patterns of the 10-hour mechanically milled powders in the Figure 16 below reveal considerable peak broadening and a decrease in peak intensity, indicating nanocrystalline structures and lattice strain caused by high-energy ball milling. All three alloys show α -Al (FCC) as the dominant phase, with characteristic peaks at 2θ values of $\sim 38^\circ$, 44° , 65° , and 78° , corresponding to (111), (200), (220), and (311) planes, respectively. Al-4Mn-1,2Zr (Base Alloy) consists primarily of α -Al with traces of intermetallic such as Al_3Zr , Al_6Mn , Al_4Mn . Peak broadening suggests reduced crystallite size ($\approx 20\text{--}30$ nm estimated via W-H equation).

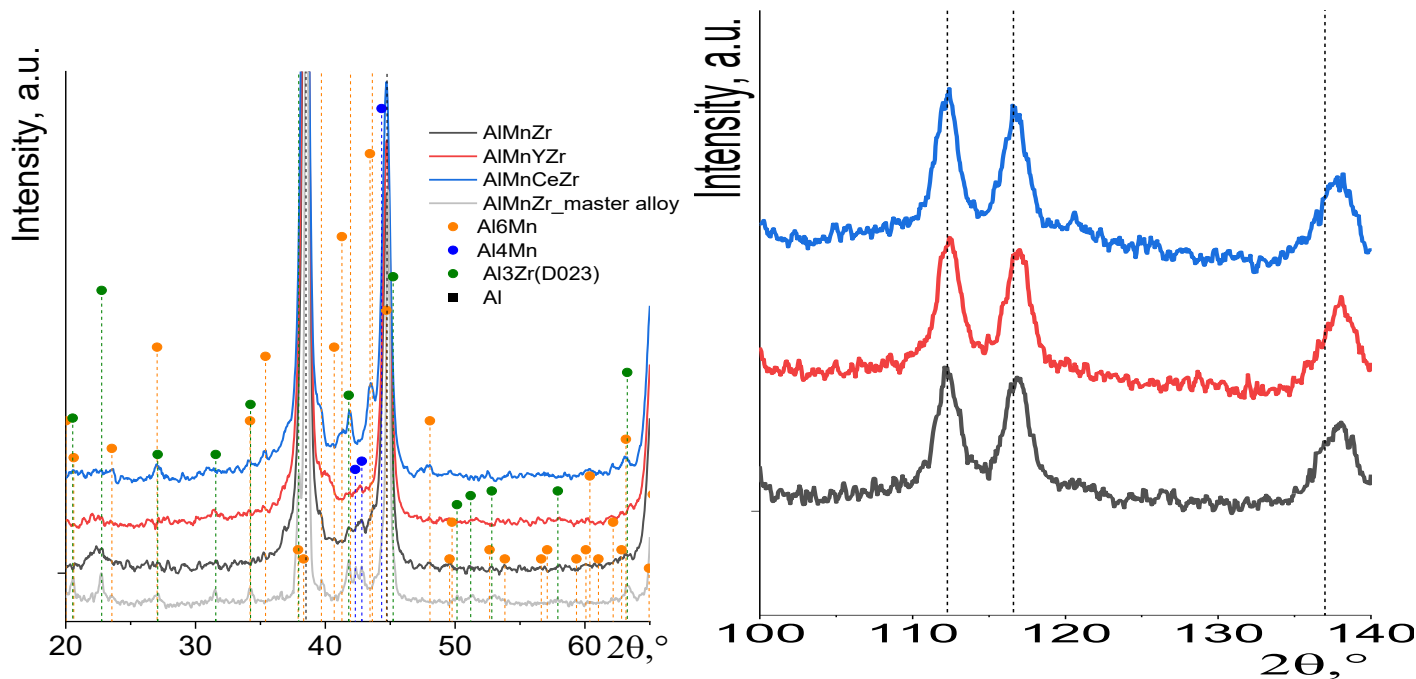


Figure 16 – XRD representation of alloys milled alloys

Microhardness of powder particles

Microhardness measurements were performed after sintering the mechanically alloyed Al-Mn-Zr and Al-Mn-Zr-RE (Y and Ce) alloys under varied HPS circumstances to evaluate their mechanical behavior. The parameters evaluated were HPS temperature of (350 and 450), annealing temperature (350, 400, and 450 °C), and duration (up to 4 hours). The initial powder values for the alloys are illustrated in the Table 3 below the effect of these characteristics on hardness is examined independently for each alloy system.

Table 3 – Initial powder particles micro hardness values

Alloy	Microhardness (HV)
Al-Mn-Zr	265 ± 8
Al-Mn-Zr-Y	240 ± 5
Al-Mn-Zr-Ce	230 ± 4

Analysis of the sintered alloys

Density of the Sintered Alloys

Figure 17 illustrates Density values for the alloys after sintering at 350 and 450 °C

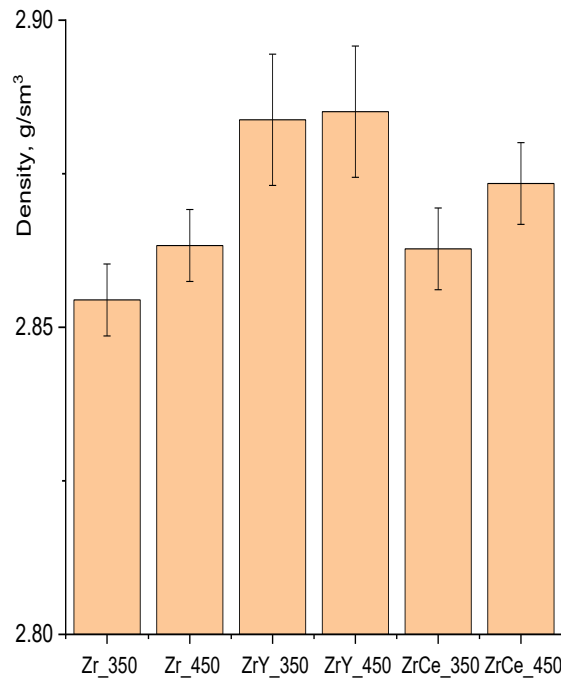


Figure 17 – Density values for the alloys after sintering at 350 and 450 °C

Densities of the alloy were measured before and after annealing of the sintered samples. After 2 hours of annealing at 450 °C, the Al-Mn-Zr alloy's density increased from 2.85 to 2.87 g/cm³, indicating pore removal. Similarly, Al-Mn-Zr-Y increased from 2.87 to 2.89 g/cm³, showing enhanced densification after annealing.

XRD for sintered alloys

The XRD patterns of the compressed and sintered alloys as illustrated in Figure 18 below it reveals significant microstructural change post-milling. Heat treatment between 350 °C and 450 °C promotes recovery and recrystallization with growth of the crystallite size, the development of intermetallic phases, and lattice strain relaxation. Al-4Mn-1,2Zr shows clearer and sharper α -Al peaks, indicating grain growth and stress release. Stable Al₃Zr and Al₆Mn phases were observed, suggesting diffusion-controlled precipitation.

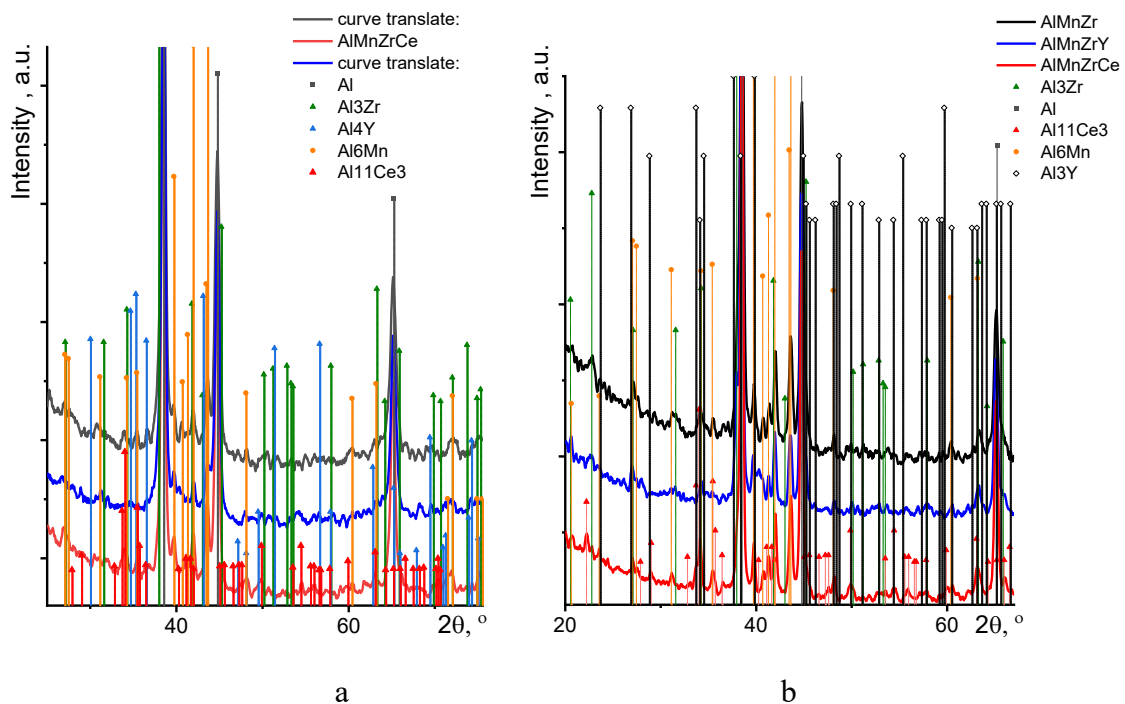


Figure 18 –XRD representation of alloys compacted at 350 °C (a) and 450 °C (b)

The XRD patterns of the Al-Mn-Zr-RE alloys sintered at 350 and 450 °C indicate that FCC-Al matrix is present in all the samples with intermetallic compounds Al_3Zr , Al_3Y and $Al_{11}Ce_3$ formed. Peak broadening at 350 °C was higher and secondary peaks intensity was smaller indicating nanocrystalline and strained structures were developed with incomplete phase precipitation. Conversely, 450°C pressing raises the crystallinity and sharpens intermetallic peaks, which means better phase development and less lattice strain. These findings clearly show that, higher compaction pressures enhance the degree of phase formation completeness and stabilization of intermetallic dispersion, which are pivotal mechanical performance and thermal stability of these advanced aluminum alloys.

The stability of these phases post-annealing, especially after 2 and 4 hours, supports the structural integrity of the alloy system under thermal exposure. XRD analysis revealed the formation of various intermetallic phases during mechanical alloying and hot pressing. The key diffraction peaks identified as α -Al, Al_6Mn , and Al_3Zr phases. Samples with Ce and Y exhibited extra peaks for $Al_{11}Ce_3$ and Al_3Y phases.

Microhardness of sintered sample

The Al-Mn-Zr alloy sample consolidated at 450 and annealed at 400 °C (450HPS@400) had the highest microhardness across all circumstances tested. This is due to the synergistic effect of high compaction pressure and enough heat activation, which promotes improved atomic diffusion, densification, and the creation of a uniform ultrafine-grained structure. These results are consistent with [37] [24] findings on densification behavior and diffusion-enhanced sintering in mechanically alloyed Al-based systems. The 350HPS@350 °C condition exhibited the second highest hardness. Despite the lower compaction pressure, the lower sintering temperature aided in maintaining a refined microstructure with minimal grain coarsening. The 350HPS@450 °C sample had the lowest measured hardness. This is most likely due to rapid grain development and probable partial recrystallization at high temperatures, as reported by [20] which reduce dislocation density and hardness. These results show that for Al-Mn-Zr, intermediate temperature (400 °C) with high sintering at (450°C) provides the best compromise between densification and microstructural refinement.

The Al-Mn-Zr-Y alloy originally exhibited maximum hardness at 450HPS@400 °C, but decreased after 2 hours of sintering. This can be attributable to grain coarsening and a drop in dislocation density caused by recovery processes. Yttrium, a rare earth metal, works as a powerful grain boundary stabilizer and refiner, although extended exposure to high temperatures can reduce its effectiveness [62]. The 350HPS@350 °C condition had the second highest hardness, with values comparable to the 450HPS@400 °C. This result supports the findings of [43] who emphasize the importance of controlled thermal exposure for maximizing hardness in mechanically alloyed systems. The 350HPS@450 °C sample had the lowest hardness, indicating the negative impact of high temperature at low compaction pressure, potentially due to inadequate consolidation and excessive grain growth.

In the Al-Mn-Zr-Ce system, 350HPS@350 °C produced the maximum hardness, followed by 350HPS@400 °C and 450HPS@400 °C. Interestingly, the lowest hardness was achieved at 350HPS@450 °C. This pattern indicates that Ce operates differently than Y, possibly due to differences in atomic size, diffusion properties, and compound formation tendency. Cerium forms stable intermetallic, such as $Al_{11}Ce_3$, which contribute to hardness when well-dispersed and nanosized. However, high sintering temperature or duration may cause coarsening and phase segregation, limiting the strengthening effect, as shown by [63]. Moreover, low pressure combined with low-to-moderate temperatures appeared optimal in preserving the fine microstructure, indicating that Ce-containing alloys benefit more from gentler sintering conditions.

Comparative Analysis and Interpretation

A comparative summary of the hardness trends across the three alloy systems under varying HPS conditions is provided in the Figure 19 below:

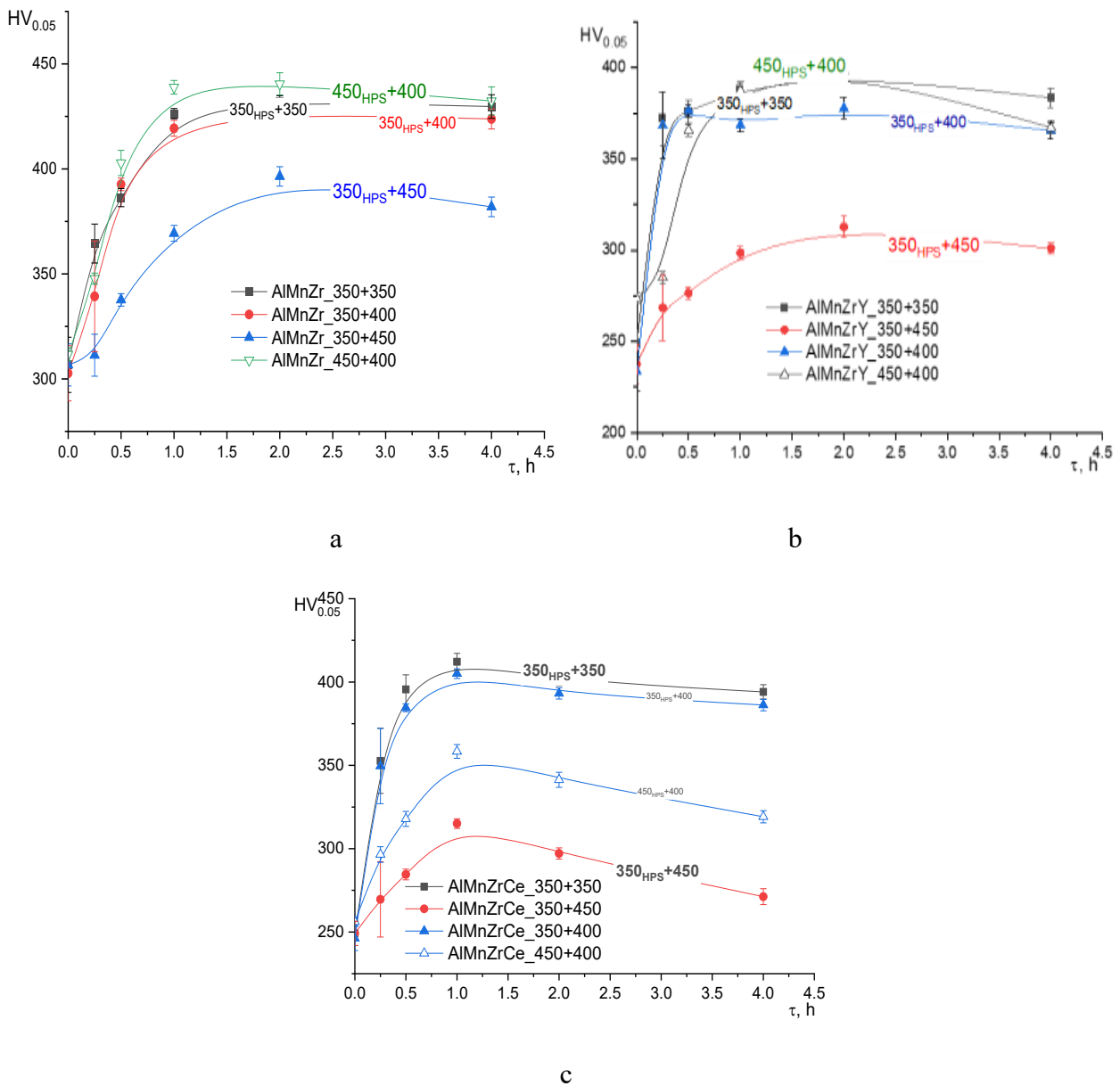


Figure 19 – Micro hardness values at different temperature of (a) Al-Mn-Zr b) Al-Mn-Zr-Y and (c) Al-Mn-Zr-Ce

The Al-Mn-Zr-Ce alloy showed moderate improvement, from an initial microhardness of 250 HV to 340 HV after 2 hours of annealing, with a corresponding macro hardness increase to 220 HV. As indicated in Table 4 below prolonged annealing to 4 hours resulted in a slight reduction, indicating potential over-aging effects

Table 4 – Hardness values before and after annealing.

Alloy	Condition	Microhardness (HV)	Hardness (HV)
Al-Mn-Zr	Sintered	280 ± 15	210 ± 10
Al-Mn-Zr	Annealed 2h @ 450°C	440 ± 20	400 ± 15
Al-Mn-Zr-Y	Sintered	250 ± 5	200 ± 8
Al-Mn-Zr-Y	Annealed 2h @ 450°C	300 ± 15	230 ± 10
Al-Mn-Zr-Ce	Sintered	260 ± 12	190 ± 9
Al-Mn-Zr-Ce	Annealed 2h @ 450°C	345 ± 18	230 ± 10

The mechanical properties of the alloys were assessed using microhardness and hardness tests. The as-pressed Al-Mn-Zr sample had a microhardness of 300 HV and a hardness of 210 HV, which rose dramatically after annealing at 450 °C for 2 hours to 440 HV and 400 HV, respectively. The increased hardness is due to fine grain strengthening and homogenous particle distribution. Al-Mn-Zr-Y samples had significantly lower starting values (250 HV microhardness), but after annealing, the hardness increased to 400 HV (micro) and 230 HV (macro), confirming the yttrium-induced grain boundary pinning.

Hardness values significantly improved after hot pressing and annealing, especially at 450 °C. Initial microhardness for Al-Mn-Zr, Al-Mn-Zr-Y, and Al-Mn-Zr-Ce were 279.6, 249.5, and 256.2 HV respectively. After annealing for 2 hours Annealing at 4 hours showed a slight reduction in values, indicating thermal softening due to over-aging or grain growth. As shown by comparison of the three alloys with their respective hardness values

Microstructural Analysis

SEM examination employing Backscattered Electron (BSE) imaging was performed to evaluate the microstructural evolution of Al-Mn-Zr-based alloys (with Ce, Y) subjected to Hot Press Sintering (HPS) at 350 and 450 MPa, both before and after 4 hours of annealing. The micrographs indicated significant variations in grain shape and elemental dispersion.

350HPS Compact (Before Annealing) The microstructure consisted of tiny, somewhat agglomerated granules scattered uniformly throughout the matrix. The EDS elemental maps in figure below showed a homogeneous distribution of Mn, Zr, Ce, and Y, indicating effective alloying during mechanical milling (10 hours). Fe contamination from grinding pots was minimal (~0.1-0.2%), in line with [50] findings.

350HPS Compact (After 4 Hours of Annealing) After annealing, substantial grain development and smoother interfaces were observed, as indicated in Figure 20 below indicating thermally triggered diffusion and partial coalescence. Small Mn-rich precipitates appeared, indicating the early stages of phase segregation, as previously observed in binary Al-Mn alloys [50].

The higher compaction pressure resulted 450HPS Compact (Before Annealing) in a denser and more refined structure with well-defined grain boundaries and minimal porosity. Granules remained fine, and the matrix showed excellent cohesiveness, indicating increased densification due to greater HPS.

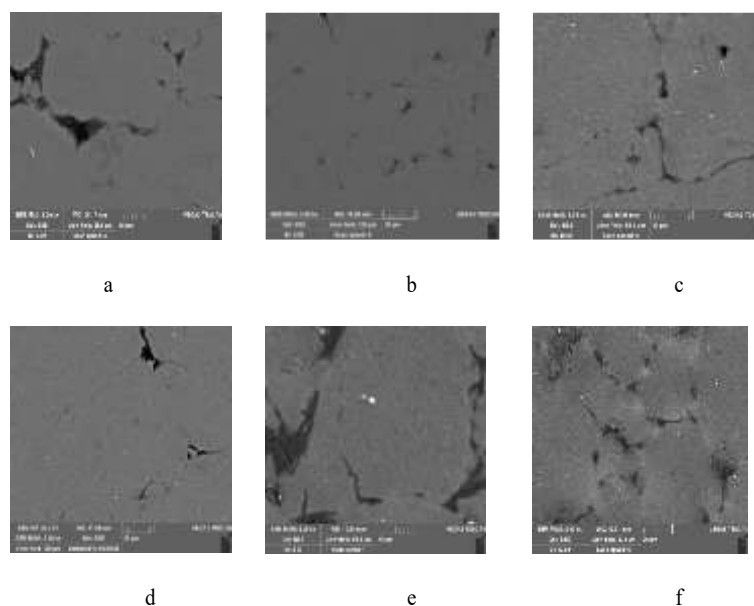
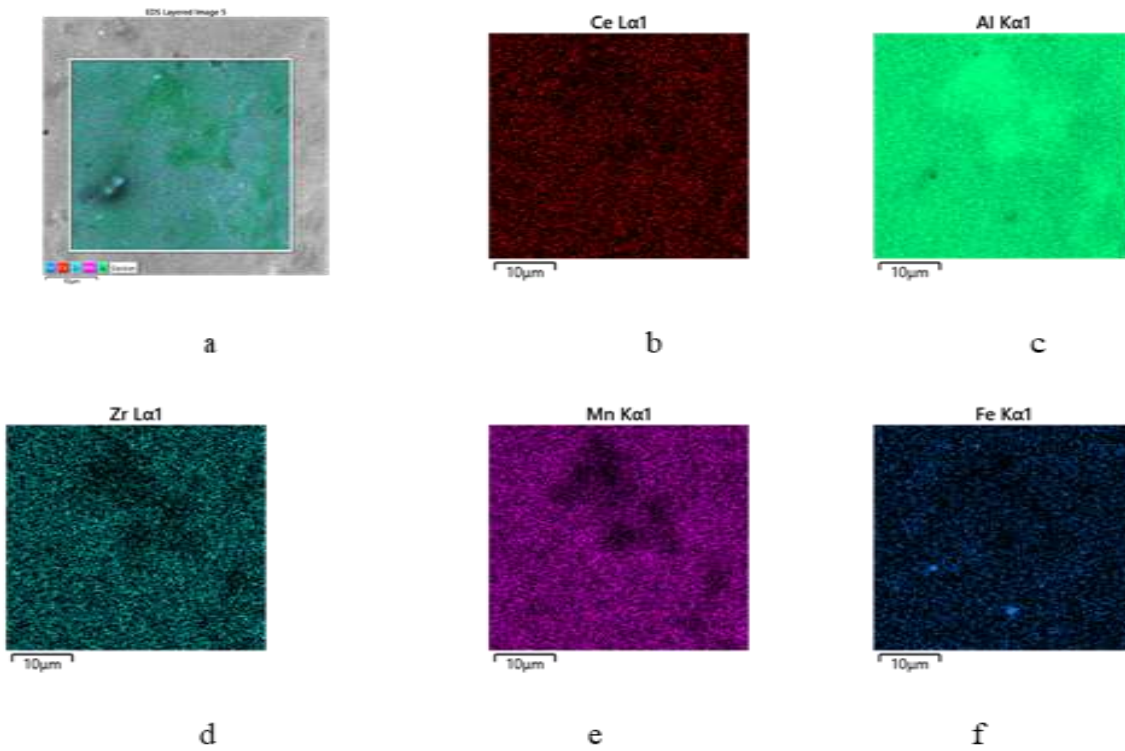


Figure 20 – SEM-BSE Images of a) Al-Mn-Zr , b) Al-Mn-Zr-Ce c) Al-Mn-Zr-Y 350HPS before Annealing and d) Al-Mn-Zr e) Al-Mn-Zr-Ce f) Al-Mn-Zr-Y 350HPS after Annealing



450HPS Compact (After 4 Hours of Annealing) Annealing increased observable coarsening and the creation of intermetallic-rich zones, as illustrated in figure 21 below especially in Mn and Ce areas. Despite the increased particle size, the elemental distribution remained relatively uniform. This result is consistent with the findings of [16] [15] who found that RE additions impacted grain boundary stability and increased heat resistance.

EDS Mapping and Phase Distribution

Elemental distribution in 350 and 450 HPS alloys are shown in Figure 21.

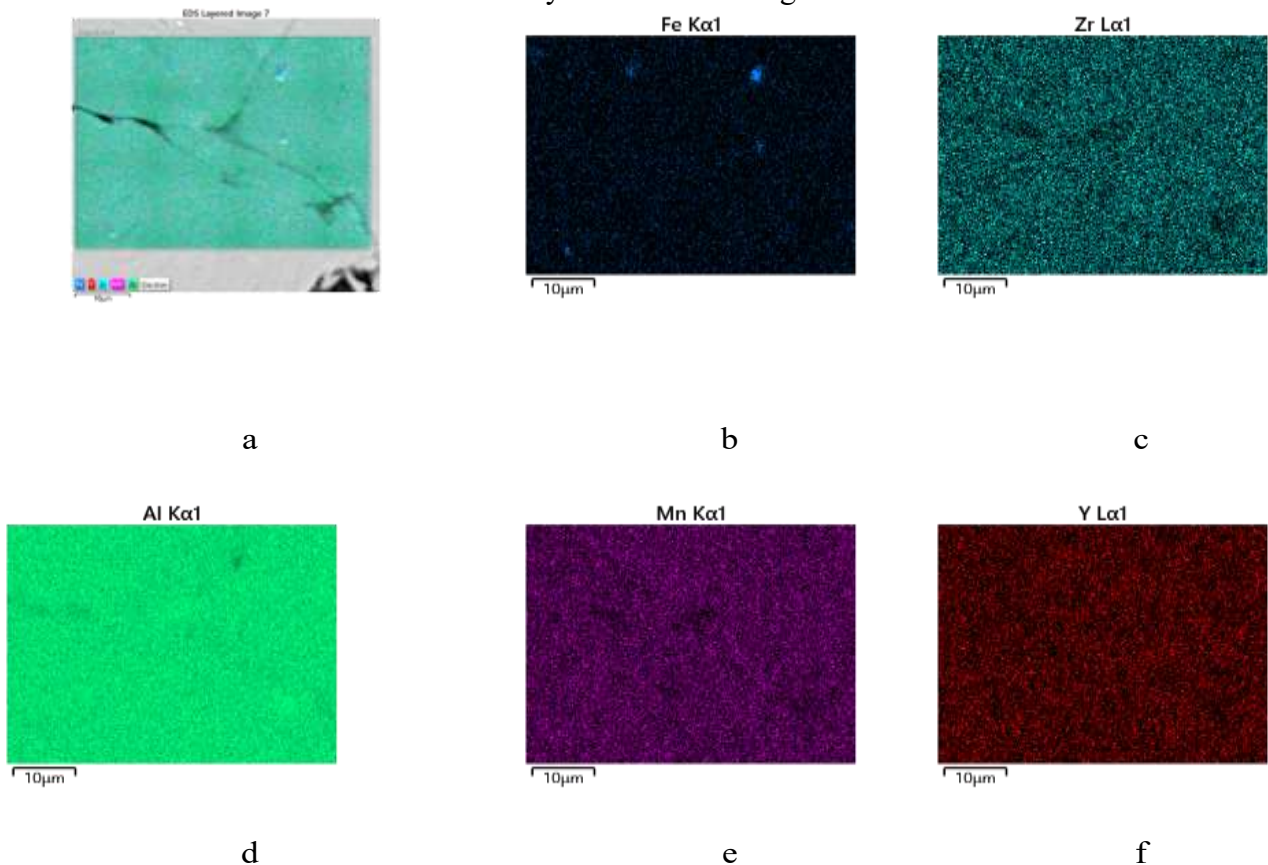


Figure 21 – Elemental distribution in 350 and 450 HPS alloys (a)EDS Image (b) Fe; (c) Zr (d) Al (e) Mn (f)

The elemental distribution of Mn, Zr, Ce and Y is consistent across all samples. Minor Fe contamination (~0.1-0.2 vol%) is consistent with earlier literature [20] possibly due to steel balls and vials used in high-energy milling.

Mechanical Properties

The mechanical properties at compression tests for Al-Mn-Zr-RE alloys processed via 350 MPa and 450 MPa HPS was evaluated at both room and elevated temperature: Table 5 below shows that the strength properties at room and higher temperature for both 350 and 450 HPS levels.

Table 5 – The mechanical properties after 10 hours MA and annealing for 350 ,400 and 450 temperatures

Alloy	Sintering/ Annealing Temperature (°C)	Tests at 20 °C			Tests at 350 °C	
		$\sigma_{0.2}$, MPa	σ_{max} , MPa	ψ , %	YS, MPa	ψ , %
Al-4Mn-1,2Zr	350/350	639±7	695±10	1.4±0.2	290±10	7.2±0.8
	350/400	585±5	641±7	1.4±0.2	265±5	11±1
	350/450	567±10	639±7	1.6±0.2	237±5	12±2
	450/400	766±10	881±5	2.4±2	321±10	7±2
Al-4Mn-1,2Zr-0,6Ce	350/350	590±10	945±7	43±3	102±5	44±5
	350/400	574±5	990±5	42±3	97±5	45±4
	350/450	547±7	987±6	42±3	94±5	45±5
	450/400	670±10	733±10	17±2	121±10	22±2
Al-4Mn-1,2Zr-0,6Y	350/350	684±5	877±10	27±3	198±10	42±2
	350/400	606±5	777±10	25±5	136±10	43±2
	350/450	540±10	762±5	25±5	132±10	44±2
	450/400	648±5	698±7	19±2	139±10	12±2

The strength of Al-Mn-Zr alloys additions of Ce and Y showed a great variation with regard to composition and thermal treatment. The Ce-containing alloy (Al-4Mn-1,2Zr-0,6Ce) showed the highest ultimate tensile strength (UTS) of up to 990 MPa at room temperature (20 °C) after 350/400 °C treatment and outstanding ductility ($\psi = 42-45\%$), which is indicative of its high strain-hardening ability and refined microstructure. The Y-modified alloy (Al-4Mn-1,2Zr-0,6Y) exhibited balance between strength and ductility, having UCS equal to 698 and 877 MPa and moderate plasticity. Conversely, the plain Al-4Mn-1,2Zr alloy exhibited the lowest ductility, ($\psi < 3\%$, in most conditions and the highest UCS of 881 MPa at 450/400 C. All alloys showed lower strengths, but higher elongation at the high temperature (350 °C), with the Ce-modified alloy retaining a combination of high strength (up to 121 MPa YS) and high ductility ($\psi = 45\%$). This data points to the strengthening effect of Ce addition in aluminum alloys as a major factor increasing ductility without reducing UTS, therefore holding promise as an addition to high-performance, thermally stable aluminum alloys.

CONCLUSIONS

This study successfully demonstrates the synthesis, and characterization of high-alloyed Al-Mn-Zr-RE (Y, Ce) alloys fabricated through mechanical alloying and hot press sintering. By systematically varying the rare earth (RE) content and employing different sintering and annealing conditions, established a strong correlation between microstructural evolution, phase transformations, and the resulting mechanical and thermal properties. A detailed study that includes XRD examination, granule morphology, and microhardness and microstructure analyses shed light on phase evolution, mechanical behavior and microstructural stability of the prepared alloys.

1. XRD indicated that supersaturated with Mn and Zr solid solutions was formed due to dissolution of alloying elements in the aluminum matrix after 10h of mechanical alloying while residual Al_4Mn phase were observed in the Al-Mn-Zr and Al-Mn-Zr-Y alloys, and Al_6Mn formed in the Al-Mn-Zr-Ce alloy. SEM examination of the granule morphology showed that particles had been homogeneously distributed with fine agglomeration. Nanostructured grains of the (Al) and precipitates of intermetallic phases formed after mechanical alloying, hot press sintering and annealing/aging processes at 350-450 °C and these factors contributed to the improved properties.
2. SEM investigations revealed that Ce, Y, Zr, and Mn were homogeneously distributed in the alloy matrix after milling and precipitation free zones formed during hot press sintering. Minor residual Fe contamination (~0.1–0.2 %) from the milling media, as determined by the detection of Fe in the as-fabricated alloys, which agreed to previous literature and not expected to have a substantial effect on alloy performance.
3. Microhardness results showed that samples sintered at 450 aged at 400°C were the hardest, indicating that higher press sintering temperature and moderate annealing/aging temperature have effectively promoted a low cavitation with precipitated strengthening without significant grain growth. Although the hardness decreased slightly with extended annealing for 4 h in the alloys with rare earth elements, caused by grains and precipitates coarsening.
4. The Al-Mn-Zr alloy demonstrated a high strength at ambient and elevated temperatures yield strength of 760 and 320 MPa and reduced ductility with 2,4 and 7% at room and 350 °C respectively. Additional alloying with Y and Ce decreased yield strength while improved ductility for the similar treated alloys.

The stated results prove that the synergistic effects of alloying elements and high energy ball milling, with the appropriate hot press sintering, make the alloys studied better at tolerating high temperatures and more resistant to destruction.

RECOMMENDATIONS AND RESEARCH IMPLICATIONS

1. Optimize Rare Earths: Evaluate different contents and combinations of RE elements (e.g., Er, Gd, La) in order to fine-tune phase distribution and mechanical properties.
2. Mechanical Property Profiling: Expand testing to tensile, fatigue, and creep behavior at elevated temperatures for aerospace and energy sectors.
3. Oxidation and Corrosion Behavior: Investigate the surface stability of the alloys in oxidizing and corrosive atmospheres to justify their potential use.
4. Demonstration of these superalloys in industrial practice Develop industrial application of these optimized alloy systems.

In summary, this work provides a solid foundation for the design of advanced Al-based alloys with superior structural and thermal properties, demonstrating the promising potential of mechanical alloying and hot press sintering in next-generation material development.

REFERENCES

1. Flower H High Performance Materials In Aerospace, Springer Science and Media, 2012.
2. Gegel G Enabling technology for the design of short-fiber reinforced aluminum MMC components, vol. 1, International Journal of Metalcasting, 2007, pp. 57-67.

3. Raiendrachari S "An overview of high-entropy alloys prepared by mechanical alloying followed by the characterization of their microstructure and various properties," *Alloys*, 2022 vol. 1, no. 2, pp. 116-132,.
4. E A. Starke, J T Staley "Application of modern aluminum alloys to aircraft," *Progress in Aerospace Sciences* , 1996 vol. 32, no. 2-3, pp. 131-172,.
5. J. Yang, Z. Zhu, S. Han, Y. Gu, Z. Zhu and H. Zhang, "Evolution Limitations Advantages and future challenges of magnesium alloys as materials for aerospace applications," *Journal of Alloys and compounds* , 2024 vol. 1008,.
6. W.S Miller, L. Zhuang, J. Bottema, A. Witterbood, P. Smet, A. Haszler and A. Vieregge, "Recent development in Aluminium alloys for the automotive industry," *Materials Science and Engineering* , 2000. vol. 280, no. 1, pp. 37-49,
7. Rajan j "DEVELOPMENT OF ULTRAFINE GRAINED A356 ALUMINIUM ALLOY BY SEVERE PLASTIC DEFORMATION AND STUDIES ON ITS DEFORMATION BEHAVIOUR AND MACHINABILITY," 2017. vol. 10.13140, no. RG.2.2.12032.74241,
8. R Lumley, "Introduction to aluminium metallurgy. In Fundamentals of aluminium metallurgy," Woodhead Publishing, 2011. vol. 1, pp. 1-19,
9. Yakovtseva OA, Emelina NB, Mochugovskiy AG, Bazlov AI, Prosviryakov AS, Mikhaylovskaya AV "Effect of Mechanical Alloying on the Dissolution of the Elemental Mn and Al-Mn Compound in Aluminum," *Metals*, 2023. vol. 13, no. 1765,
10. Y. H. J. a. Martin J, "3D printing of high-strength aluminium alloys," *Nature*, 2017 vol. 549, pp. 365-369,.
11. M. A. Z. M. G. I. Mochugovskiy AG, "Effect of heat treatment on the grain size control, superplasticity, internal friction, and mechanical properties of zirconium-bearing aluminum-based alloy," *Journal of Alloys and Compounds*, 2021. vol. 5,
12. L. D. Nam S.W, "The effect of Mn on the mechanical behavior of Al alloys," *Metals and Materials*, 2000. vol. 6, no. 1, pp. 13-16,
13. A. F. A. M. W. Buso S.J., "Characterization by TEM of a Supersaturated P/M Al-Mg-Zr Alloy after Thermal Treatments," *Material Science Forum*, 2003 Vols. 426-432, pp. 4179-4184,.
14. H. J, "Aluminium in innovative light-weight car design," *Materials transactions*, 2011 vol. 5, pp. 818-24,.
15. S. K. Prosviryakov AS, "Strengthening of mechanically alloyed Al-based alloy with high Zr contents," *Materials Science and Engineering* , 2018 Jan 24. vol. 713, pp. 174-9,
16. Mikhaylovskaya AV, Kishchik AA, Tabachkova NY, Prosviryakov AS, Mochugovskiy AG "Influence of secondary Quasicrystalline I-phase precipitates on the grain structure and mechanical properties of the Al-Mg-Mn Alloy," *Physics of metal and Metallography* , 2022. vol. 123, no. 5, pp. 474-81,
17. Wang X, Liu J, Huang M, Zheng Y, Yang J, Li N, Dong X "A review on wear resistance of Mg alloys: the influence of common rare earth alloying elements and general modification techniques," *Materials Science and Technology*, 2024. p. 02670836241262597,
18. Raabe D, Ponge D, Uggowitzer PJ, Roscher M, Paolantonio M, Liu C, Antrekowitsch H, Kozeschnik E, Seidmann D, Gault B, De Geuser F, "Making sustainable aluminium by recycling scrap. The science of "dirty" alloys,," *Progress in Materials science* , 2022 Jul 1. vol. 128, p. 1000947,
19. Zheng Q. "Recent Progress on Regulating Strategies for the Strengthening and Toughening of High-Strength Aluminum Alloys," *Materials*, 2022. vol. 15(13), p. 4725,
20. Yakovtseva O.A. et al "Effect of high-energy ball milling on the microstructure, phase composition and microhardness of the Al-Mn-Cu alloy," *Izvestiya Vuzov Tsvetnaya*.
21. Rana RS, Purohit R, Das S "Reviews on the influences of alloying elements on the microstructure and mechanical properties of aluminum alloys and aluminum alloy composites," *International Journal of Scientific and research publications*, 2021 Jun 6. vol. 6, no. 2, pp. 1-,

22. Yakovtseva O.A. et al "Influence of Pre-Milling on the Mn Solid Solubility in the Al-Mn-Cu Alloy during Mechanical Alloying," *Metals*(Basel), 2023 vol. 13, no. 4, p. 756,.
23. Cai Z, Liu H, Wang R, Peng C, Feng Y, Wang X "Microstructure and mechanical properties of the extruded Al-Cu-Mn-Sc-Zr alloy during single-stage and two stage aging.," *Journal of Materials Engineering and Performance* , 2023 Jan vol. 32, no. 1, pp. 185-98,.
24. Suryanarayana C "Mechanical alloying and milling.," *Progress in materials science*, 2001 Jan 1 Vols. (1-2), no. 46, pp. 1-84,.
25. Buso S.J., Almeida Filho A., Monteiro W.A. "High temperature Si-Ge alloy towards thermoelectric applications," *A comprehensive review Materials Today Physics*, 2021. vol. 21,
26. Benjamin J.S "Dispersion strengthened superalloys by mechanical alloying.," *Metallurgical transaction*, 1970 Oct 1. pp. 2943-51,
27. R. W. Cahn "Materials Science and Technology A Comprehensive Treatment," ed. Haasen P.K.J Wiley- VCH, 1996 vol. 15, pp. 220-400,.
28. Soni, P. R. "Application of surface active substance in mechanical alloying," *Materials Science and Engineering*, 1991 vol. 134, pp. 1346-1349,.
29. Shingu P.H., Ishihara K.N "Metastable melting phenomena and solid state amorphization(SSA) by mechanical alloying," *J Alloys Compd*, 1993 vol. 2, pp. 319-324,.
30. Alves, A. K., Bergmann, C. P., & Berutti, F. A. "High-Energy Milling In Novel Synthesis and Characterization of Nanostructured Materials," *Engineering Materials Springer Berlin Heidelberg*, vol. 10, pp. 978-3-642-41275-2-7, 2013.
31. Joy J, Krishnamoorthy A, Tanna A, Kamathe V, Nagar R, Srinivasan S, "Developments on the Synthesis of Nanocomposite Materials Via Ball Milling Approach for Energy Storage Applications," *Applied Sciences*, vol. 12(18), p. 9312, 2022.
32. Murty BS, Ranganathan S, Rao MM "Solid State amorphization in binary Ti-Ni, Ti-Cu and ternary Ti-Ni-Cu system by mechanical alloying," *Materials Science and Engineering* , vol. 149, no. 2, pp. 231-240, 1992.
33. Eckert J, Schultz L, Urban K Formation of quasicrystalline and amorphous phases in mechanically alloyed Al-based and TiNi-based alloys, *Acta Metallurgica et Materialia*, 1991. vol. 39, no. 7, pp. 1497-1506,
34. Pabi SK, Joardar J, Manna I, Murty BS. Nanocrystalline phases in Cu Ni, Cu · Zn and Ni Al systems by mechanical alloying. *Nanostructured Materials*. 1997 Jan 1;9(1-8):149-52..
35. Liu ZG, Guo JT, Ye LL, Li GS, Hu ZQ. Formation mechanism of TiC by mechanical alloying. *Applied physics letters*. 1994 Nov 21;65(21):2666-8..
36. Klassen T, Herr U, Averbach RS. Ball milling of systems with positive heat of mixing: Effect of temperature in Ag-Cu. *Acta materialia*. 1997 Jul 1;45(7):2921-30
37. Benjamin JS, Volin TE. The mechanism of mechanical alloying. *Metallurgical transactions*. 1974 Aug;5(8):1929-34.,
38. Koch CC, Kim MS. The structure of amorphous alloys synthesized by mechanical alloying-non glass forming systems. *Le Journal de Physique Colloques*. 1985 Dec 1;46(C8):C8-573..
39. Davis RM, McDermott B, Koch CC. Mechanical alloying of brittle materials. *Metallurgical Transactions A*. 1988 Dec;19:2867-74.
40. Benjamin J.S "Mechanical alloying — A perspective," *Metal Powder Report*, vol. 45, no. 2, pp. 122-127, 1990.
41. Lee PY, Koch CC. Formation of amorphous Ni-Zr alloys by mechanical alloying of mixtures of the intermetallic compounds Ni₁₁Zr₉ and NiZr₂. *Applied physics letters*. 1987 Jun 1;50(22):1578-80.
42. Gilman PS, Benjamin JS. Mechanical alloying. *Annual review of materials science*. 1983 Aug;13(1):279-300.

43. Aikin BJ, Courtney TH. The kinetics of composite particle formation during mechanical alloying. *Metallurgical transactions A*. 1993 Mar;24:647-57.
44. Aikin BJ, Courtney TH, "Modeling of Particle Size Evaluation During Mechanical Milling," *Metallurgical Transactions A*, 1993 vol. 24, no. 11, pp. 2465-2471.
45. Aikin BJ, Courtney TH, Maurice DR. Reaction rates during mechanical alloying. *Materials Science and Engineering: A*. 1991 Nov 15;147(2):229-37.
46. Yavari AR. Phase transformations in nanocrystalline alloys. *Materials Science and Engineering: A*. 1994 May 1;179:20-6.
47. Bordia RK, Camacho-Montes H. Sintering: fundamentals and practice. *Ceramics and Composites Processing Methods*. 2012 Apr 6:1-42
48. Kang SJ. Sintering: densification, grain growth and microstructure. Elsevier; 2004 Nov 27..
49. Chan KF, Zaid MH, Mamat MS, Liza S, Tanemura M, Yaakob Y. Recent developments in carbon nanotubes-reinforced ceramic matrix composites: A review on dispersion and densification techniques. *Crystals*. 2021 Apr 21;11(5):457.1 .
50. Yakovtseva OA, Mochugovskiy AG, Prosviryakov AS, Bazlov AI, Emelina NB, Mikhaylovskaya AV. The microstructure and properties of Al–Mn–Cu–Zr alloy after high-energy ball milling and hot-press sintering. *Metals*. 2024 Mar 6;14(3):310..
51. Fecht HJ, Hellstern E, Fu Z, Johnson WL. Nanocrystalline metals prepared by high-energy ball milling. *Metallurgical Transactions A*. 1990 Sep;21:2333-7.
52. Yavari AR. Metastable and nanocrystalline polymorphs of magnetic intermetallics. *Materials Science and Engineering: A*. 1997 Jun 15;226:491-7.
53. Yavari AR "Mechanically Prepared Nanocrystalline Materials," *Materials Transactions, JIM*, , 1995 vol. 36, no. 2, p. 228–239.
54. Li S, Wang K, Sun L, Wang Z. A simple model for the refinement of nanocrystalline grain size during ball milling. *Scripta metallurgica et materialia*. 1992 Aug 15;27(4):437-42..
55. Witkin DB, Lavernia EJ. Synthesis and mechanical behavior of nanostructured materials via cryomilling. *Progress in Materials Science*. 2006 Jan 1;51(1):1-60..
56. Naik SN, Walley SM. The Hall–Petch and inverse Hall–Petch relations and the hardness of nanocrystalline metals. *Journal of Materials Science*. 2020 Mar;55(7):2661-81..
57. Darling KA, Roberts AJ, Armstrong L, Kapoor D, Tschopp MA, Kecskes LJ, Mathaudhu SN. Influence of Mn solute content on grain size reduction and improved strength in mechanically alloyed Al–Mn alloys. *Materials Science and Engineering: A*. 2014 Jan 1;589:57-65.
58. Lei Z, Wen S, Huang H, Wei W, Nie Z. Grain refinement of aluminum and aluminum alloys by Sc and Zr. *Metals*. 2023 Apr 12;13(4):751..
59. Ding W, Zhao X, Chen T, Zhang H, Liu X, Cheng Y, Lei D. Effect of rare earth Y and Al–Ti–B master alloy on the microstructure and mechanical properties of 6063 aluminum alloy. *Journal of Alloys and Compounds*. 2020 Jul 25;830:154685..
60. Wang X, Liu J, Huang M, Zheng Y, Yang J, Li N, Dong X. A review on wear resistance of Mg alloys: the influence of common rare earth alloying elements and general modification techniques. *Materials Science and Technology*. 2025 Jun;41(8):570-91..
61. Yang J, Zhu Z, Han S, Gu Y, Zhu Z, Zhang H. Evolution, limitations, advantages, and future challenges of magnesium alloys as materials for aerospace applications. *Journal of Alloys and Compounds*. 2024 Sep 25;176707..
62. Suryanarayana C "Evolution of mechanical alloying, Editor(s): Shashanka Rajendrachari, *Mechanical Alloying of Ferrous and Non-Ferrous Alloys*," Elsevier, 2024. pp. 1-37,
63. Courtney TH, Maurice D. Process modeling of the mechanics of mechanical alloying. *Scripta Materialia*. 1996 Jan 1;34(1):5-11

64. Davis RM, McDermott B, Koch CC. Mechanical alloying of brittle materials. *Metallurgical Transactions A*. 1988 Dec;19:2867-74.
65. Weeber AW, Bakker H. Amorphization by ball milling. A review. *Physica B: Condensed Matter*. 1988 Oct 1;153(1-3):93-135.
66. M. B. Nie JF, "Comments on the "dislocation interaction with semicoherent precipitates (ω phase) in deformed Al-Cu-Mg-Ag alloy," *Scripta Materialia*., vol. 1:42, no. 4, pp. 409-13., 2000 Jan 3.
67. Ringer SP, Hono K. Microstructural evolution and age hardening in aluminium alloys: atom probe field-ion microscopy and transmission electron microscopy studies. *Materials characterization*. 2000 Jan 1;44(1-2):101-31..
68. Sankaran KK, Mishra RS. *Metallurgy and design of alloys with hierarchical microstructures*. Elsevier; 2017 Jun 14..